Background gluon field effects in photon production from the quark–gluon plasma

Эффекты фонового глюонного поля в рождении фотонов КГП

Aleksei Nikolskii

S. Nedelko, V. Voronin, A. Snigirev, V. Goloviznin, G. Zinovjev,

Seminar «Theory of hadronic matter under extreme conditions»

BLTP JINR, 24.06.2026

Presentation Outline

- Key papers ;
- Motivation ;
  - experimental signatures of the formation of quark–gluon matter ;
  - electromagnetic signals of the quark–gluon plasma (QGP) ;
  - the *puzzle* of direct photons and the enhanced dilepton yield ;
- Synchrotron radiation of quarks in a gluon field ;
  - classification of radiation mechanisms ;
    - chromoelectric flux-tube model ;
  - main features of our approach ;
  - radiation spectrum ;
- Photon production via the process $gg \to \gamma$ as a signal of deconfinement ;
    - domain model of the QCD vacuum and hadronization ;
  - conversion $gg \to \gamma$ in the confinement phase ;
  - photon production $gg \to \gamma$ in the deconfinement phase ;
- Conclusions and discussion ;

Key papers

Papers relevant to this talk

- V.V. Goloviznin, A.V. Nikolskii, A.M. Snigirev, and G.M. Zinovjev, *Probing confinement by direct photons and dileptons*, Eur. Phys. J. A 55: 142, (2019), arXiv: 1804.00559 ;
- S. Nedelko, A. Nikolskii, *Photons production in heavy-ion collisions as a signal of deconfinement phase*, Eur. Phys. J. A 59 4, 70, (2023), arXiv: 2208.00842 ;
- V.V. Goloviznin, A.V. Nikolskii, A.M. Snigirev, and G.M. Zinovjev, *Synchrotron radiation as a probe of confinement and QGP,* PoS HardProbes *2018* (2018) 175 Contribution to: HP2018, 175 ;
- Sergei Nedelko, Aleksei Nikolskii, *Photons as a Signal of Deconfinement in Hadronic Matter under Extreme Conditions*, MDPI Physics 5 (2023) 2, 547-553 ;
- S.N. Nedelko, A.V. Nikolskii, *Photons as Probes of Deconfinement in Quark-Gluon Plasma,* Phys.Part.Nucl.Lett. 20 (2023) 5, 1153-1156 ;

Motivation

Experimental signatures of quark–gluon matter formation

- Hydrodynamic (collective) properties of the medium :
  - anisotropic flow: v_2, v_3 … ;
  - two-particle azimuthal correlations (long-range «ridge» effect) ;
  - low shear viscosity $\eta/s \approx 1/4\pi$ (ideal gas $\Longrightarrow$ almost perfect liquid) ;
- Energy loss of quarks and gluons in the medium :
  - jet quenching ;
  - spectral asymmetry in *jet+jet, γ+jet* , and *Z+jet* processes ;
  - modification of the internal structure of hadronic jets ;
- Color-charge screening in the medium :
  - suppression of quarkonium production (J/ψ , Υ) ;
  - regeneration and anisotropic flow of «soft» J/ψ ;
- Strangeness enhancement :
  - enhanced production of strange particles ($\mathrm{K}, \Lambda, \Xi, \Omega$) в AA / (pp and pA) collisions ;
- Electromagnetic signals (probes) :
  - prompt photons, «*direct photon flow puzzle*» ;
  - dileptons ;
  - «specific» mechanisms of photon production ;

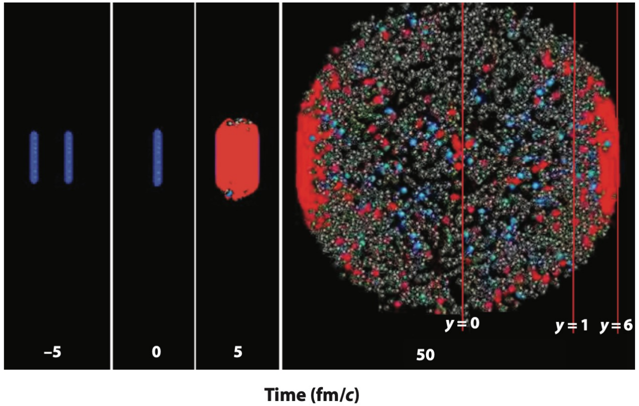

Wit Busza, Krishna Rajagopal, Wilke van der Schee, *Ann.Rev.Nucl.Part.Sci*. 68 339-376 (2018)

Motivation / EM probes QGP: photons and dileptons

Electromagnetic probes, signals QGP: photons and (di)leptons

Sources of **photons** in pp and AA collisions:

- decay photons: $m \to \gamma + X, m = \pi^0, \eta, \eta', \omega, a_1, \ldots$ *Dominate the in the inclusive photon spectrum*.
- direct photons: obtained by subtracting the decay-photon contribution from the experimentally measured inclusive photon spectrum. They are commonly classified as follows:
  - high-p_T («hard») photons ($p_T \geq 4-5$ GeV): «prompt» photons produced in initial hard NN collisions, jet fragmentation - pQCD process, and jet-medium photons: $q_{\text{hard}} + q(g)_{\text{QGP}} \to \gamma + q(g)$.
  - low-p_T : photons emitted by the thermalized QGP and from hadronic interactions :
    - «thermal» photons are produced through $q\bar{q}$ annihilation: $q + \bar{q} \to g + \gamma$ and Compton scattering: $q(\bar{q}) + g \to q(\bar{q}) + \gamma$. Calculated within LO and NLO pQCD LO methods;
    - hadronic sources are related to:
      - secondary meson interactions: $\pi + \pi \to \rho + \omega$, $\rho + \pi \to \pi + \gamma$, $\pi + K \to \rho + \gamma$, …

        These processes are typically evaluated using effective field-theory models, transport models, and hydrodynamic approaches.
      - hadronic bremsstrahlung, such as meson–meson (mm) and meson–baryon (mB): $m_1 + m_2 \to m_1 + m_2 + \gamma$, $m + B \to m + B + \gamma$, $m = \pi, \eta, \rho, \omega, \mathrm{K}, \mathrm{K}^*$, $B = \mathrm{p}, \Delta, \ldots$

        Here the leading contribution corresponds to the radiation from one charged hadron scattered off a neutral hadron.

- Wit Busza, Krishna Rajagopal, Wilke van der Schee, *Ann.Rev.Nucl.Part.Sci*. 68 339-376 (2018) ;
- E. L. Bratkovskaya, *Phenomenology of photon and dilepton production in relativistic nuclear collisions*, Nucl. Phys. A 931 194-205 (2014), Proceedings Quark Matter 2014.

Motivation / direct photons

Direct photons were first measured in the WA80 (S+Au, $\sqrt{s} \approx 19$ GeV) and WA98 (Pb+Pb, $\sqrt{s} = 17.3$ GeV) experiments at CERN.

- R. Albrecht et al. (WA80 Collaboration), Phys. Rev. Lett. 76 (1996) 3506;

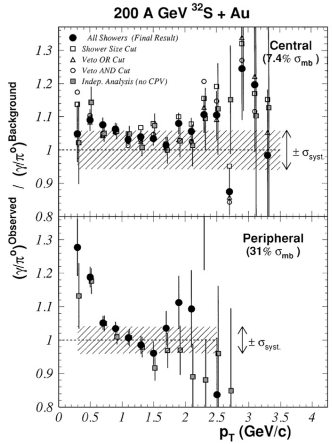

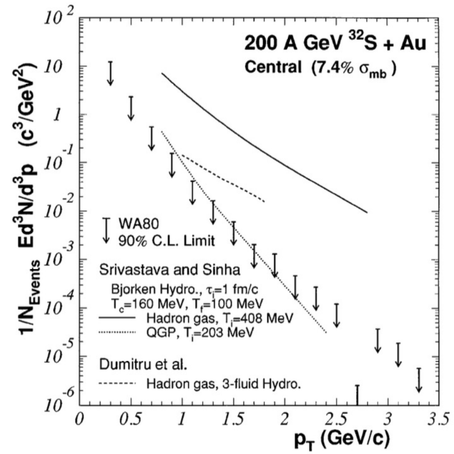

Unexpectedly high direct-photon yield

- M.M. Aggarval et al. (WA98 Collaboration), Phys. Rev. Lett. 85 (2000) 3595.

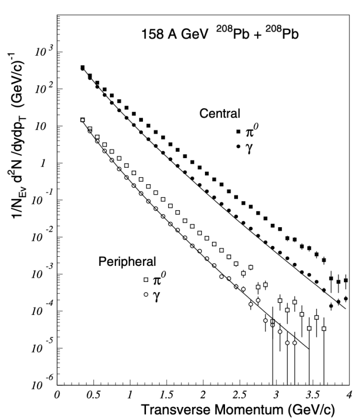

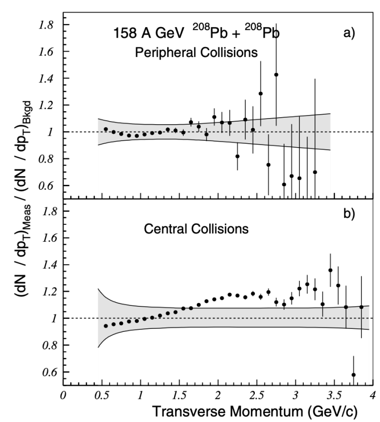

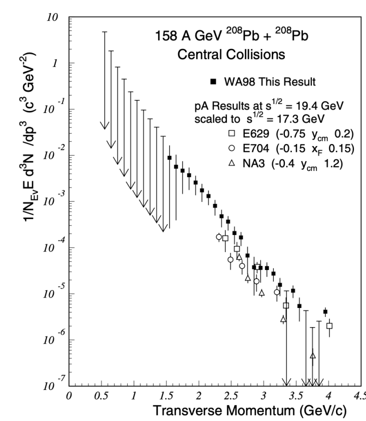

Motivation / direct photons

Subsequently, the PHENIX collaboration at RHIC (BNL) measured direct photons in Au+Au collisions at $\sqrt{s}$ =200 GeV.

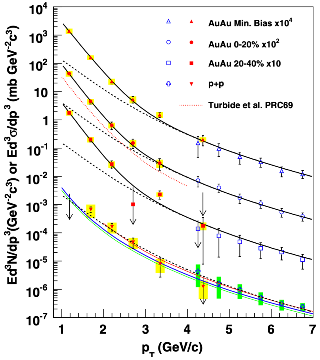

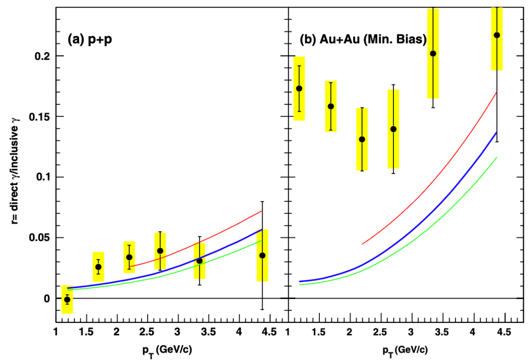

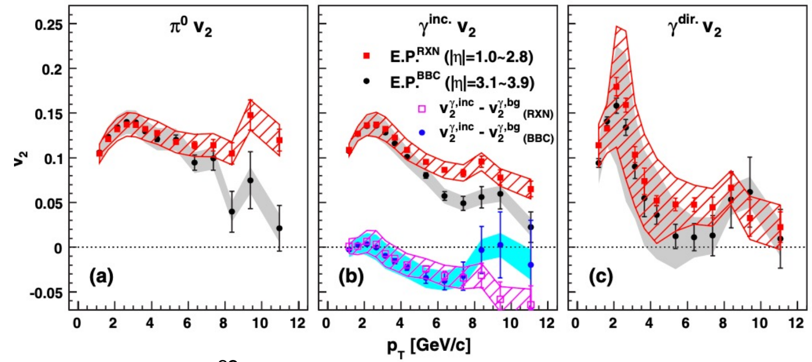

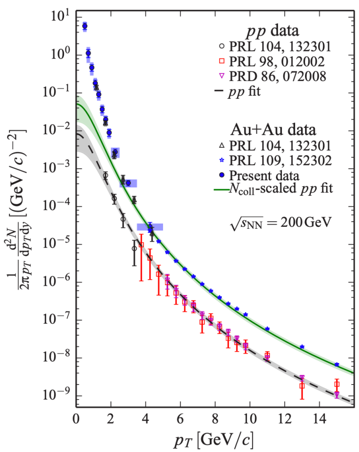

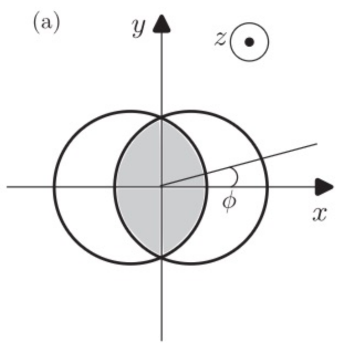

$$\frac{dN}{d\phi} \approx \left(1 + \sum_{n=1}^{\infty} 2v_n \cos n(\phi)\right) \quad , v_n = \langle \cos n\,(\phi) \rangle.$$

$$v_2^{\gamma\ \mathrm{dir}} = \frac{\sum_i v_2^{\gamma\ i} N_i^{\gamma}}{\sum_j N_j^{\gamma}}.$$

Direct photons:
v_2 puzzle or
direct photons flow puzzle.

Early emission of photons from the hot QGP $\Longrightarrow$ expected small v_2.
Experiment: large v_2, almost as large as for hadrons.

- S. Voloshin and Y. Zhang, *Z. Phys. C* 70, 665 (1996) ;
- A. Adare et al. (PHENIX Collaboration). *Phys. Rev. Lett*. 104, 132301 (2010) ;
- A. Adare et al. (PHENIX Collaboration). *Phys. Rev. Lett*. 109, 122302 (2012) ;
- A. Adare et al. (PHENIX Collaboration). *Phys. Rev. C* 91, 064904 (2015).

Motivation / direct photons

ALICE collaboration (LHC) in Pb+Pb at $\sqrt{s}$ =2.76 TeV and p+p $\sqrt{s}$ =13 TeV collisions .

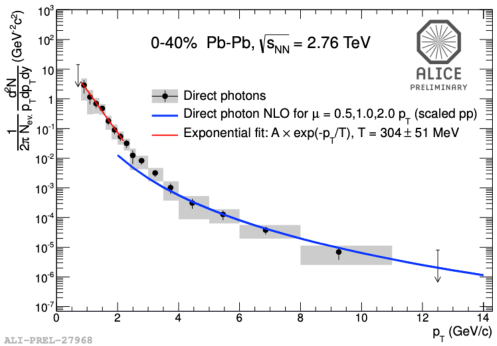

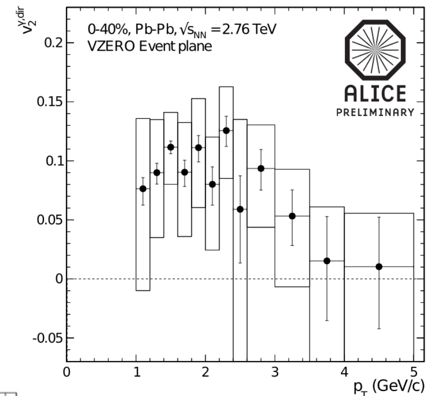

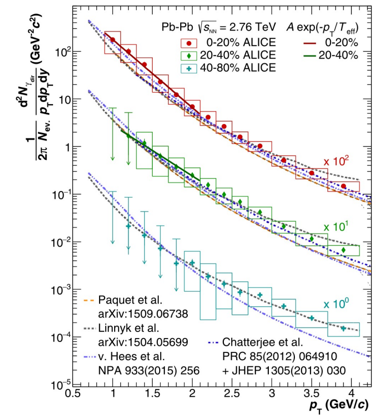

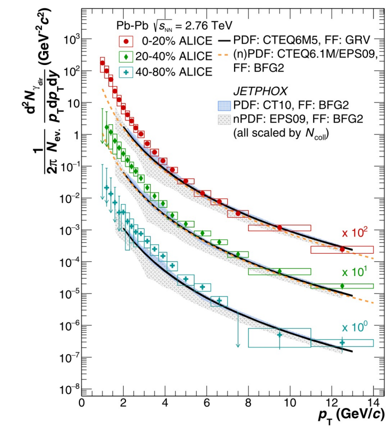

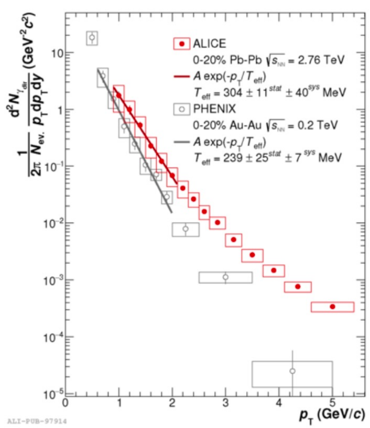

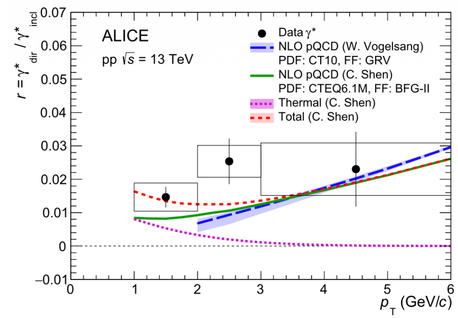

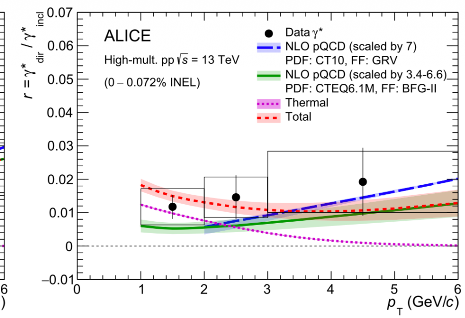

- Daniel Lohner and the ALICE Collaboration, *J. Phys.: Conf. Ser.* 446 012028 (2013) ;
- J. Adam et al. (ALICE Collaboration). *Phys.Lett.B* 754 235-248 (2016) ;
- M. Germain and the ALICE Collaboration, *Nucl.Phys.A* 967 696-699 (2017) ;
- S. Acharya et al. (ALICE Collaboration), *Phys.Lett.B* 868 139645 (2025) .

Motivation / lepton pairs - dileptons

Can be emitted at all stages of the reaction. A key feature: ad. «degree of freedom» - inv. mass of the pair M.
Production of **dileptons** in pp, pA, AA collisions:

- hadronic sources:
  - low M ($M < 1$ GeV/c) – Dalitz decays of mesons and baryons ($\pi^0, \eta, \Delta, \ldots$) ; direct decays of vector mesons (ρ, ω, ϕ), and hadronic bremsstrahlung ;
  - intermediate M ($1 < M < 3$ GeV/c) – contributions from $D + \overline{D}$ pairs, and multi-meson reactions ($\pi + \pi$, $\pi + \rho$, $\pi + \omega$, $\rho + \rho$, $\pi + a_1, \ldots$) – so-called «4π» contributions ;
  - high M ($M > 3$ GeV/c) – direct decay of vector mesons (J/Ψ , Ψ') and «hard» Drell–Yan annihilation ($q + \bar{q} \rightarrow l^+ + l^-$) .
- «thermal» QGP dileptons:
  - dominantly contribute in the intermediate M ($1 < M < 3$ GeV/c) and are related to interactions of quarks and gluons in the medium. The leading contributions are «thermal» $q\bar{q}$ annihilation: $q + \bar{q} \rightarrow l^+ + l^-$ and QCD Compton scattering: $q(\bar{q}) + g \rightarrow q(\bar{q}) + l^+ + l^-$.

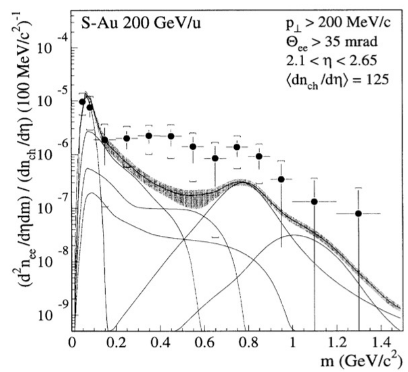

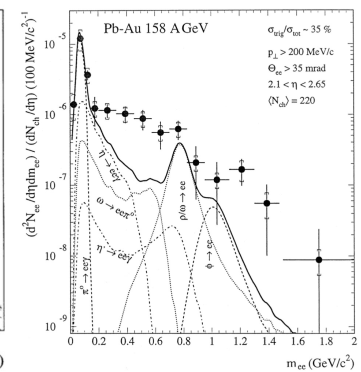

- G. Agakichiev et al. (CERES Collaboration). *Phys.Rev.Lett.* 75 1272-1275 (1995) ;
- G. Agakichiev et al. (CERES/NA45 Collaboration). *Phys.Lett.B* 422 405-412 (1998) ;
- E. L. Bratkovskaya, *Nucl. Phys. A* 931 194-205 (2014), Proceedings Quark Matter 2014.

First results on the lepton «excess».

Motivation / lepton pairs - dileptons

PHENIX and STAR experiments (RHIC, BNL), p+p and Au+Au collisions $\sqrt{s}$ =200 GeV.

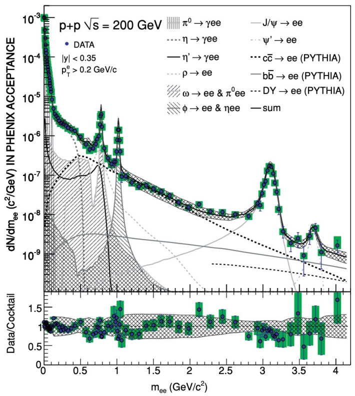

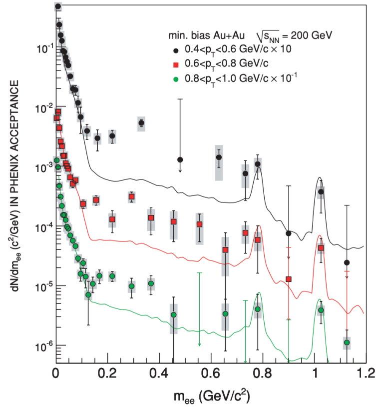

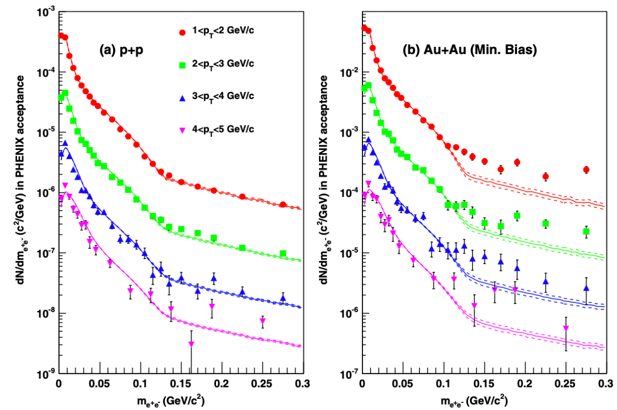

Total contribution from hadronic sources is small compared to the measurements.

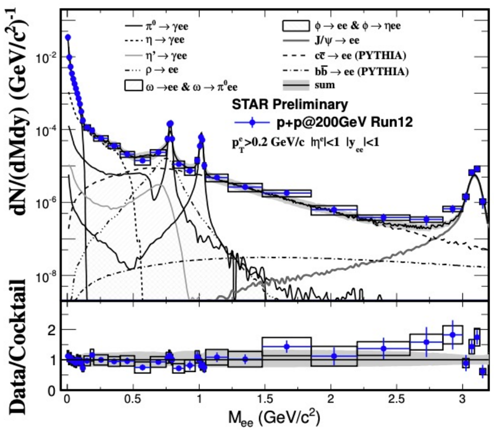

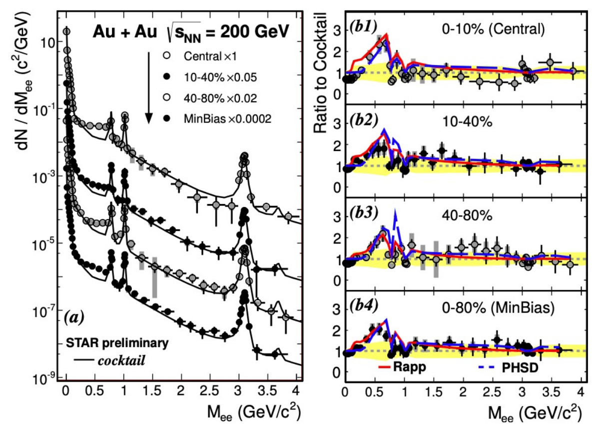

- A. Adare et al. (PHENIX Collaboration). *Phys.Rev.Lett.* 104 132301 (2010) ;
- A. Adare et al. (PHENIX Collaboration). *Phys.Rev.C* 81 034911 (2010) ;
- Yi Guo et al. (STAR Collaboration). *J.Phys.Conf.Ser.* 535 012006 (2014) .

Motivation / EM probes QGP: photons and dileptons

EM probes weakly interact with medium – provide direct information about the processes inside the «fireball», but are experimentally difficult to measure and extract from the background.

- **Photons:** anomalously large yield and directed flow – large v_2 in $p_T \leq 4$ GeV .
  - Models that successfully describe hadronic spectra (hydrodynamic approaches, transport models such as PHSD, DQPM) fail to simultaneously reproduce the photon spectra.
  - Photon production from QGP shows a stronger centrality dependence compared to photons from the hadronic gas.
- **Dileptons:** anomalously large signal in $M \leq 3$ GeV compared to the hadronic «cocktail» expectation.
  - low M (< 1 GeV) – contribution from in-medium vector meson decays (especially ρ) is enhanced.
  - for $M > 1$ GeV – thermal dileptons dominate: spectrum slope $\exp(-p_T/T_{\text{eff}})$, isotropic angular distribution.

- **Experiment:** in both cases, an enhancement is observed in the most central collisions, especially in the region $p_T, M \leq 3$ GeV .
- **Possible additional sources** of EM signals in QGP at $p_T \leq 4$ GeV: deconfinement dynamics, strong (chromo)EM fields, surface effects, glasma stage, thermal radiation, non-perturbative effects, and hadronic bremsstrahlung. Early stages of the reaction also contribute via pre-equilibrium effects and initial flow development.

iNSPIRE HEP

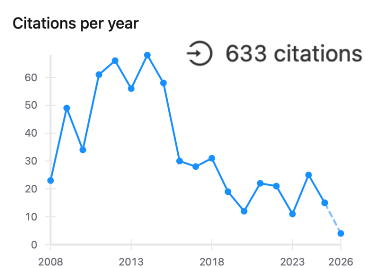

NICA
Nuclotron-based Ion Collider fAcility

Synchrotron radiation of quarks

Synchrotron radiation of quarks

- Intense EM radiation of magnetic bremsstrahlung type (synchrotron radiation) is generated by the **interaction of quarks with gluon field responsible for their confinement in the QGP**.
  - Bremsstrahlung – EM radiation emitted by a charged particle when it is scattered (decelerated) in an electric field. For example: $e^- + Z \to e^- + Z + \gamma$. Spectrum $\sim 1/\omega$, broad and continuous, with the maximum determined by the particle energy. Example: X-ray tube.
  - Synchrotron radiation – EM radiation emitted by a relativistic charged particle moving along a **curved trajectory**, i.e., undergoing acceleration perpendicular to its velocity. Spectrum is characterized by a critical frequency determined by the curvature radius (R), narrow cone of radiation $\theta \sim 1/\gamma$, higher degree of polarization than bremsstrahlung radiation.

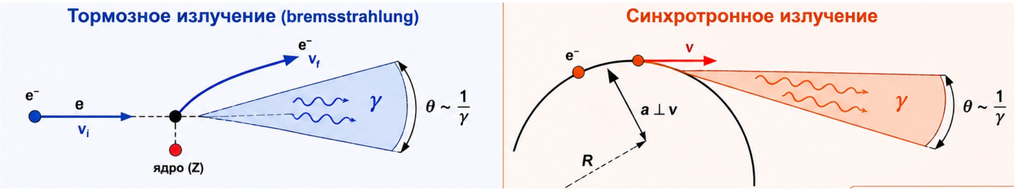

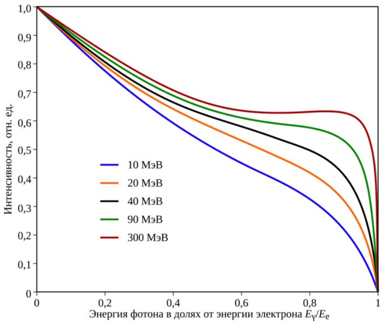

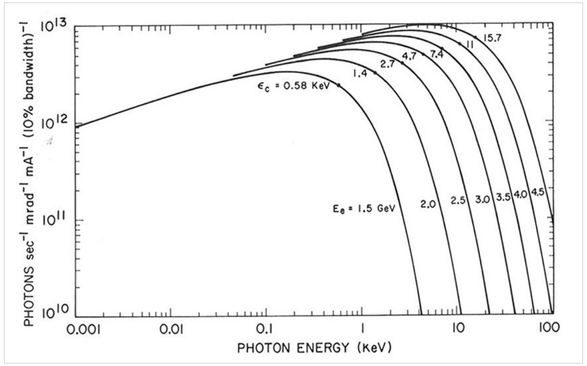

- Jackson J. D., *Classical Electrodynamics* — M.: MIR, 2002 ;
- Landau and E.M. Lifshitz., *Classical theory of fields* (Vol. II) ;
- Sokolov A.A., Ternov I. M., *Relativistic effects in Synchrotron radiation*. — M.: Nauka, 1983. — 296 p.

Synchrotron radiation of quarks

Main conditions for the existence of synchrotron radiation from quarks:

- The presence of light relativistic quarks in the QGP volume ;
- A quasiclassical character of quark motion ($R \gg \lambda_{dB}^{q}$) ;
- Confinement ;

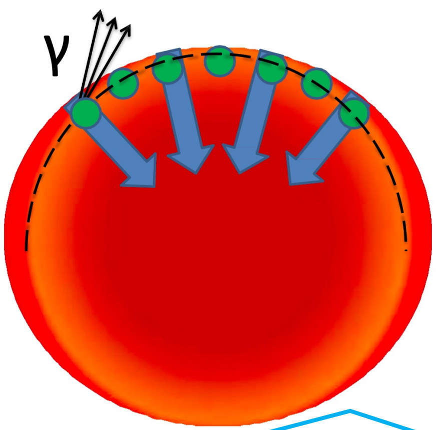

Confinement → a constant restoring force σ =0.2 GeV^2, directed along the normal to the fireball «surface».

A «surface-induced» mechanism of photon production in the QGP.

At the plasma boundary, a quark (antiquark) follows a curved trajectory. As an accelerated charged particle, it emits photons, resulting in synchrotron radiation.

- A. Casher, H. Neuberger, and S. Nussinov, *Chromoelectric-flux-tube model of particle production*, Phys. Rev. D 20 ,179-188 (1979);
- V.V. Goloviznin, A.V. Nikolskii, A.M. Snigirev, and G.M. Zinovjev, *Eur. Phys. J. A* 55: 142, (2019), arXiv: 1804.00559 ;

Backup / Chromoelectric-flux-tube model

- Confinement is realized through the formation of a chromoelectric flux tube between a $q\bar{q}$ pair ;
- The field inside the flux tube is longitudinal, homogeneous, and Abelian ;
- The energy of the flux tube grows linearly with separation: $V(r) = \sigma\, r$;
- The flux-tube parameters are the field strength E, the tube radius R, and the coupling constant g ;
- The «string tension» is given by: $\sigma = (1/2)\ E^2 \pi R^2$; and is related to the Regge slope: $\alpha = 1/(2\,\pi\,\sigma)$;
- Quark–antiquark pair production is described by the Schwinger mechanism: $w \sim \exp(-\pi m^2/gE)$;
- Hadronization proceeds through successive breaking and fragmentation of the flux tube ;

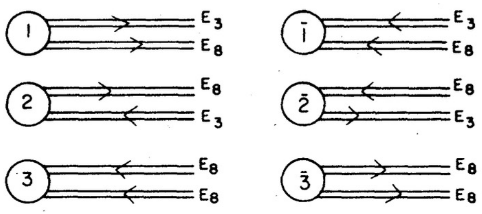

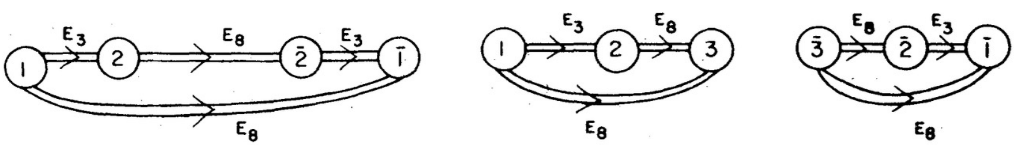

- Julian S. Schwinger, *On gauge invariance and vacuum polarization,* Phys.Rev. 82 (1951) 664-679 ;
- A. Casher, H. Neuberger, and S. Nussinov, ***Chromoelectric-flux-tube model of particle production***, Phys. Rev. D 20 ,179-188 (1979);
- B. Banerjee, N. Glendenning, T. Matsui, *Meson radiation from a quark-gluon plasma by fission of chromoelectric flux tubes,* Phys. Lett. B 127, 453 (1983);
- N. K. Glendenning, T. Matsui, *Creation of $q\bar{q}$ pairs in a chromoelectric flux tube*, Phys.Rev.D 28 2890-2891 (1983) ;
- Bo Andersson, G. Gustafson, G. Ingelman, T. Sjostrand, *Parton Fragmentation and String Dynamics,* Phys.Rept. 97 31-145 (1983) .

Synchrotron radiation of quarks

We consider the ultrarelativistic motion of a quark with energy E in the QGP volume. In the strong-field regime, characterized by σ $\left[\chi = \frac{3}{2}\frac{\sigma E}{m^3}\right]^{1/3}$ the spectral energy distribution of synchrotron radiation with respect to the photon energy ω is given by

$$\frac{dN_\gamma}{d\omega\, dt} = \frac{1}{2} e_q^2 \alpha\, \omega^{-2/3} \left(\frac{\sigma \sin\varphi}{E}\right)^{2/3}, \qquad 0 < \omega < E\,, \tag{1}$$

where $\alpha = 1/137$, e_q - quark charge, φ is the angle between the quark velocity and the normal to the plasma surface (i.e., the direction of the restoring force).

- V.V. Goloviznin, A.M. Snigirev, G.M. Zinovjev, *Z. Phys. C* 38, 255 (1988) ;

$$\frac{dI}{d\omega} \propto \omega^{1/3}$$

Relation between the spectral distribution and the energy spectrum.

$$\frac{dN}{d\omega dt} = \frac{1}{\omega}\frac{dI}{d\omega}\,, \qquad \frac{dN}{d\omega dt} \propto \omega^{-2/3}$$

- Jackson J. D., *Classical Electrodynamics* — M.: MIR, 2002 ;
- Landau and E.M. Lifshitz., *Classical theory of fields* (Vol. II) ;
- A.A. Sokolov, I. M. Ternov, *Relativistic effects in Synchrotron radiation*. — M.: Nauka, 1983.

Synchrotron radiation of quarks

Quasiclassical approach ($\lambda_{\mathrm{dB}}^{q} \ll dS$). Let the «string tension» force act along the z-axis. Then the equations of motion of a quark near the QGP boundary are given by

$$p_z = \sigma t' \,,\; p_x = p_{x_0} \,, p_y = p_{y_0},\; -p_{z_0}/\sigma \le t' \le p_{z_0}/\sigma \;, \tag{2}$$

where $p_{z_0} > 0$, p_{x_0}, p_{y_0} – are the initial values of the corresponding quark momentum components, and t'– is the proper time parameter describing the quark motion along its «trajectory».

From Eq. (1), taking into account Eq. (2), we obtain the spectral angular distribution: [motion $q \,||\, \gamma$]

$$\frac{dN_\gamma}{d\omega d\Omega} = \int_{-p_{z_0}/\sigma}^{p_{z_0}/\sigma} dt'\delta\big(\boldsymbol{n} - \boldsymbol{v}(t')\big)\, \theta[\omega < p(t')] \frac{1}{2} \frac{e_q^2 \alpha\, \sigma^{2/3}}{\omega^{2/3}} \frac{\sin^{2/3}\varphi(t')}{p^{2/3}(t')} . \tag{3}$$

Here $\boldsymbol{v}(t')$ denotes the quark velocity, $\boldsymbol{n}$ is the unit vector along the photon momentum, $p(t') = \left(p_x^2 + p_y^2 + p_z^2\right)^{1/2}$, and $\sin\varphi(t') = \left(p_x^2 + p_y^2\right)^{1/2}/p(t')$.

Integrating Eq. (3) over the initial quark momenta and taking into account a thermal quark ensemble (Boltzmann distribution), we obtain the synchrotron radiation rate per unit time dt and unit surface area dS :

$$\frac{dN_\gamma}{dS\, dt\, \omega^2 d\omega d\Omega} = \frac{3}{7} \frac{g\langle e_q^2\rangle \alpha}{(2\pi)^3\, \sigma^{1/3}} \omega^{2/3} \sin^{2/3}\varphi_0 \int_1^\infty d\xi \exp\left(-\frac{\omega}{T}\xi\right)\left(\xi^{7/3} - 1\right), \tag{4}$$

where $\langle e_q^2\rangle = e_u^2 + e_d^2$, g =6 (spin x color), T – is the plasma temperature, $\varphi_0 = \widehat{\boldsymbol{k}\,\boldsymbol{n}}$, $\xi = E/\omega$.

❑ V.V. Goloviznin, A.M. Snigirev, G.M. Zinovjev, *Z. Phys. C* 38, 255 (1988) ;

Synchrotron radiation of quarks

Total number of emitted photons:

$$\frac{dN_\gamma}{dS\,dt} = \int d\omega d\Omega \frac{dN_\gamma}{dS\,dt\,\omega^2 d\omega d\Omega} = A\langle e_q^2\rangle\alpha\, T^{11/3}\sigma^{-1/3}\,, \tag{5}$$

where $A = 3.12g \cdot 2^{5/3}\Gamma^2(4/3)/(2\pi)^2 \approx 1.2$.
For comparison with experiment in Eq. (4), we perform the change of variables $(\omega, \theta, \varphi) \to (k_\perp, x, \varphi)$:

$$\frac{dN_\gamma}{dS\,dt\,k_\perp dk_\perp} = \frac{6}{7}\frac{g\langle e_q^2\rangle\alpha {k_\perp}^{5/3}}{(2\pi)^3\,\sigma^{1/3}}\int_0^{2\pi} d\varphi \int_0^\infty dx \int_1^\infty d\xi\,(x^2+\sin^2\varphi)^{1/3}\,(\xi^{7/3}-1)\exp\left[-\frac{k_\perp(1+x^2)^{1/2}}{T}\,\xi\right], \tag{6}$$

where $x = \sinh y$, y is the rapidity, φ is the photon azimuthal angle with respect to $\boldsymbol{n}$ (or the normal to the surface of the fireball).
In the **limit** $k_\perp \gg T$, Eq. (6) takes the form:

$$\boxed{\frac{dN_\gamma}{dS\,dt\,k_\perp dk_\perp} = \mathcal{F}\langle e_q^2\rangle\,\alpha\,\sigma^{-1/3}\,{k_\perp}^{-5/6}\,T^{5/2}e^{-k_\perp/T}\,,} \tag{7}$$

где $\mathcal{F} = 0.52g \cdot 2^{1/6}\Gamma^2(5/6)\pi^{-5/2}/\Gamma(5/3)$ ≈0.29 – результат усреднения по углам θ, φ.

Synchrotron radiation of quarks

QGP evolution [J.D. Bjorken, *Phys. Rev. D* 27 (1983) 140]

$$\tau = (t^2 - z^2)^{1/2} \;\rightarrow\quad \varepsilon(\tau) = \varepsilon_0\,(\tau_0/\tau)^{4/3}, \qquad T(\tau) = T_0\,(\tau_0/\tau)^{1/3}, \qquad \rho(\tau) = \rho_0\,\tau_0/\tau\,. \tag{8}$$

in the form of a longitudinally expanding, cylindrically symmetric fireball.
Integration of Eq. (7) over the QGP surface, taking into account Eq. (8), leads to the following expression for the quark synchrotron radiation spectrum:

$$\boxed{\begin{aligned}\frac{d^2N_\gamma}{2\pi\, k_\perp dk_\perp dy} &= \int \frac{dN_\gamma}{dS\, dt\, k_\perp dk_\perp}\, r\,\tau\, d\tau = \\ &3\,\mathcal{F}\langle e_q^2\rangle\,\alpha\,(\tau_0 T_0^3)^2\, r\, {k_\perp}^{-13/3}\sigma^{-1/3}\left[\Gamma\left(\frac{7}{2};\frac{k_\perp}{T_0}\right) - \Gamma\left(\frac{7}{2};\frac{k_\perp}{T_c}\right)\right]\end{aligned}} \tag{9}$$

с учетом $\Gamma(n;\alpha_1) - \Gamma(n;\alpha_2) = \int_{\alpha_1}^{\alpha_2} dt\, t^{n-1}\, e^{-t}$.

Synchrotron radiation of quarks

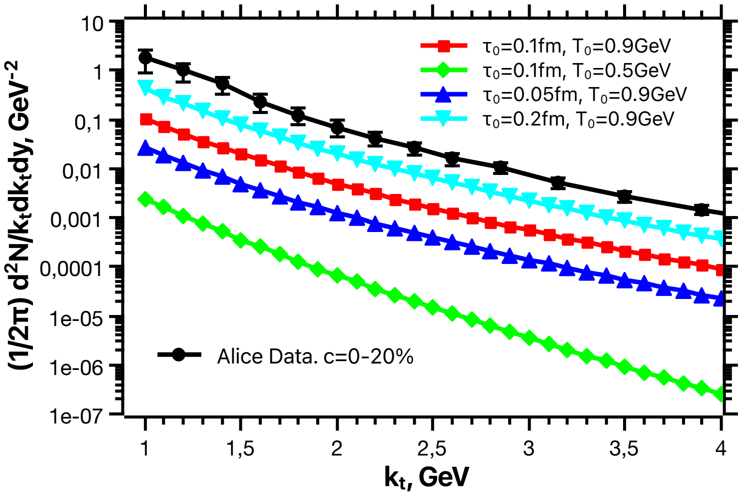

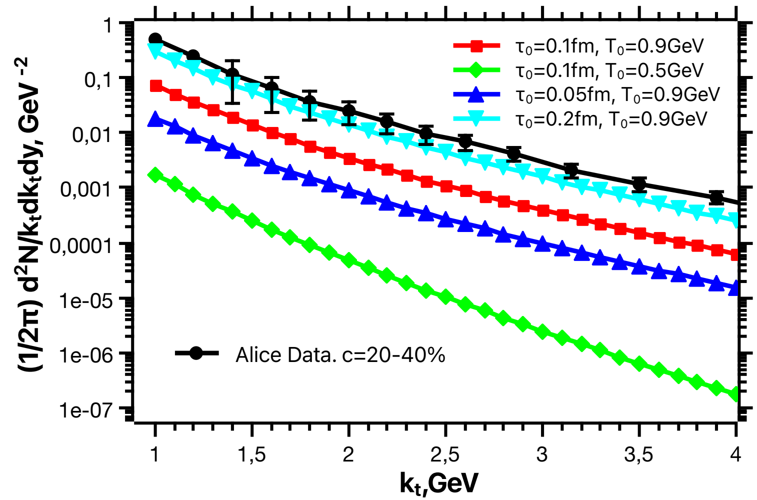

Comparison of the synchrotron radiation spectrum (Eq. (9)) from the fireball with experimental data (ALICE) for different values of τ_0 and T_0, corresponding to the onset of the hydrodynamic regime in centrality classes 0–20% (left panel) and 20–40% (right panel). The plasma system radius is $r = 10$ fm (0-20%) and $r = 7$ fm (20-40%), the phase transition temperature is $T_c = 0.2$ GeV, and the restoring force («string tension») is σ =0.2 GeV^2.

For «standard» values $\tau_0 = 0.1$ fm and $T_0 = 0.9$ GeV – the contribution amounts to approximately 10% of the experimental yield.

- ALICE Collaboration (J. Adams et al.), *Phys.Lett.B* 754 235-248 (2016).

Synchrotron radiation of quarks

Taking into account the plasma temperature gradient (from the center to the boundary) as follows from Eq. (7), within the interval τ_0 to τ_f :

$$\frac{d^2N_\gamma}{2\pi\, k_\perp dk_\perp dy} = \int \frac{dN_\gamma}{dS\, dt\, k_\perp dk_\perp}\, r\, \tau\, d\tau = \tag{10}$$

$$\mathcal{F}\langle e_q^2\rangle \alpha \frac{\tau_f^2 - \tau_0^2}{2}\, r\;\; {k_\perp}^{-5/6} T_S^{5/2} \sigma^{-1/3} \exp[-k_\perp/T_S]\,,$$

where $\tau_f = (T_0/T_C)^3 \tau_0$ is the total «lifetime» of the QGP.

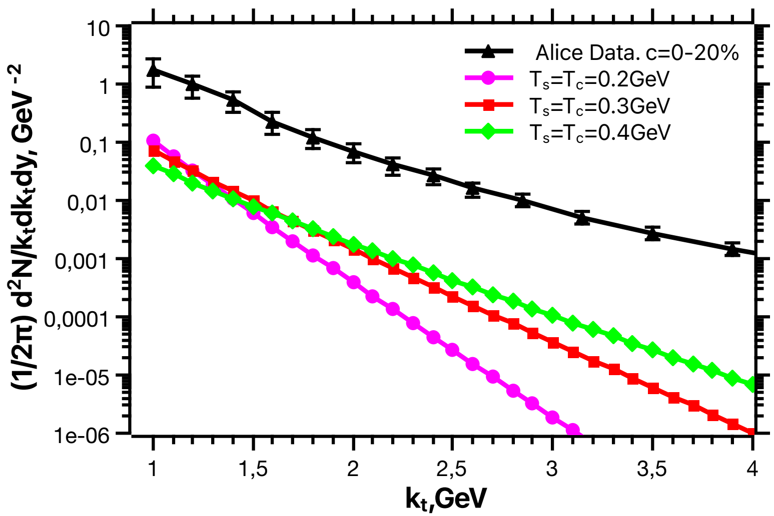

Comparison of spectrum (10) with ALICE data (0–20%) for different values of the QGP surface temperature $T_S = T_C$, $T_0 = 0.9$ GeV, τ_0 =0.1 fm.

Synchrotron radiation of quarks

Synchrotron radiation is characterized by a high degree of photon polarization. Several preferred directions can be identified: the collision axis OZ, the direction of the restoring force $\boldsymbol{\sigma} \,||\, \boldsymbol{n}$, and the photon emission direction $\widehat{\boldsymbol{k}\,\boldsymbol{n}}$. We introduce the corresponding unit vectors:

$$\boldsymbol{e}_1 = \frac{\sigma \times \boldsymbol{k}}{|\sigma \times \boldsymbol{k}|}, \qquad \boldsymbol{e}_2 = \frac{\boldsymbol{k} \times \boldsymbol{e}_1}{|\boldsymbol{k} \times \boldsymbol{e}_1|}.$$

Taking into account the linear photon polarizations along $\boldsymbol{e}_1$ и $\boldsymbol{e}_2$ the distribution (1), summed over polarizations [A.A. Sokolov, I. M. Ternov, *Relativistic effects in Synchrotron radiation*]:

$$\frac{dN_1}{d\omega\, dt} = \frac{1}{4}\frac{dN_\gamma}{d\omega\, dt}, \frac{dN_2}{d\omega\, dt} = \frac{3}{4}\frac{dN_\gamma}{d\omega\, dt}. \tag{11}$$

The polarization N_2, corresponding to the plane defined by $\boldsymbol{k}$ and $\boldsymbol{n}$ **dominates**. In the case of a cylindrically symmetric fireball (with the cylinder axis aligned with OZ), the initial degree of polarization decreases to:

$$P = \left(\frac{dN_2}{d\omega\, dt} - \frac{1}{2}\frac{dN_\gamma}{d\omega\, dt}\right) \Big/ \frac{1}{2}\frac{dN_\gamma}{d\omega\, dt} = \frac{1}{2} \tag{12}$$

down to approximately 20%:

$$\boldsymbol{P} \to \boldsymbol{P}' \approx \frac{\mathbf{1}}{\mathbf{5}}.$$

- V.V. Goloviznin, A.M. Snigirev, G.M. Zinovjev, Yad. Fiz. 48, 1826 (1988).

Synchrotron radiation of quarks

In experiments, photon polarization is practically not measured; therefore, an expression for the azimuthal distribution of (di)leptons

$$\frac{dN_\gamma}{dt\, d\Omega_1} = \frac{\alpha \mathcal{L}(P')}{2\pi k^0} \int \frac{p^2 dp}{p_1^0 (k^0 - p_1^0)} \delta[f(p)] \left[\frac{k^2 + 2\mu^2}{3} - \frac{2}{3} \boldsymbol{P'} p^2 \sin^2\theta_1 \cos 2\phi_1 \right] \quad (13)$$

was derived for the decay of a «weakly virtual» photon ($\sqrt{k} \cong \sqrt{\sigma} = 0.4$ GeV) into a lepton pair p_1, p_2 . In «thermal» $q\bar{q}$ annihilation: $q + \bar{q} \to l^+ + l^-$ and in Compton «scattering» : $q(\bar{q}) + g \to q(\bar{q}) + l^+ + l^-$ such a dependence is absent.

Synchrotron radiation may contribute to the elliptic flow coefficient v_2 (for photons and, subsequently, dileptons) due to the «distribution» of surface normals over an elliptic geometry. :

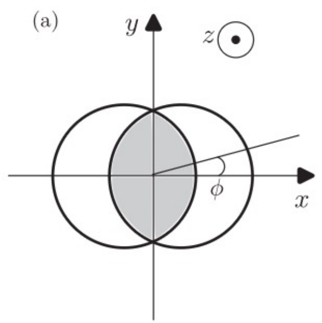

$$\int_0^{2\pi} d\phi_s \cos(2\phi_\gamma)/(2\pi) = \epsilon\,, \quad \phi_s = \tan^{-1}(y/x)\,,\ \ \phi_\gamma = (r_x/r_y)^2 \tan(\phi_s)$$

$$v_2^\gamma \propto \epsilon\,, \qquad v_2^\gamma = \frac{\int d\phi_\gamma \cos(2\phi_\gamma)(dN^\gamma/d\phi_\gamma)}{\int d\phi_\gamma (dN^\gamma/d\phi_\gamma)}\,.$$

- V.V. Goloviznin, A.M. Snigirev, G.M. Zinovjev, Yad. Fiz. 48, 1826 (1988);
- V.V. Goloviznin, A.M. Snigirev, G.M. Zinovjev, JETP Lett. 107, 527 (2018).

Synchrotron radiation of quarks

- The mechanism of photon production in the form of synchrotron radiation by quarks is a consequence of (de)confinement in the QGP, i.e. the inability of a colored object to leave the QGP ;
- The relative contribution of this radiation amounts to 10% or more of the experimental data ;
- The polarization of synchrotron photons leads to an azimuthal anisotropy of the dilepton pair ;
- Synchrotron photons contribute to the overall $v_2^{\gamma\ \mathrm{dir}}$ due to the geometric shape of the QGP .

Photons production in $gg \to \gamma$ as a signal of deconfinement

25-27; 34-45

Photons production in $gg \to \gamma$ as a signal of deconfinement

- Strong EM field in heavy-ion collisions:
- V. Skokov, A. Y. Illarionov, and V. Toneev, *Int. J. Mod. Phys. A* 24, 5925 (2009) ;
- V. Voronyuk, V. D. Toneev, W. Cassing, E.L. Bratkovskaya, V.P. Konchakovski, *Phys. Rev. C* 83, 054911 (2011) ;

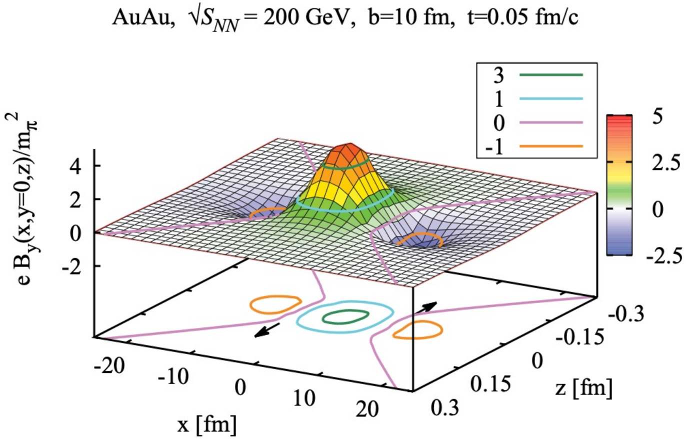

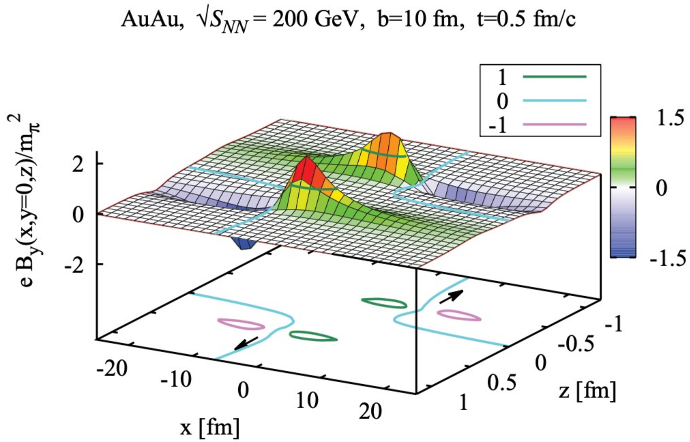

- Observable effects in the quark–gluon plasma induced by strong EM fields :
- A. Bzdak and V. Skokov, *Anisotropy of photon production: initial eccentricity or magnetic field*, Phys. Rev. Lett. 110, 192301 (2013);
- K. Tuchin, *Particle production in strong electromagnetic fields in relativistic heavy-ion collisions*, Adv. High Energy Phys. 2013, 490495 (2013);
- A. Ayala et al. *Prompt photon yield and elliptic flow from gluon fusion induced by magnetic fields in relativistic heavy-ion collisions*, Phys. Rev. D 96, 014023 (2017);

Photons production in $gg \to \gamma$ as a signal of deconfinement

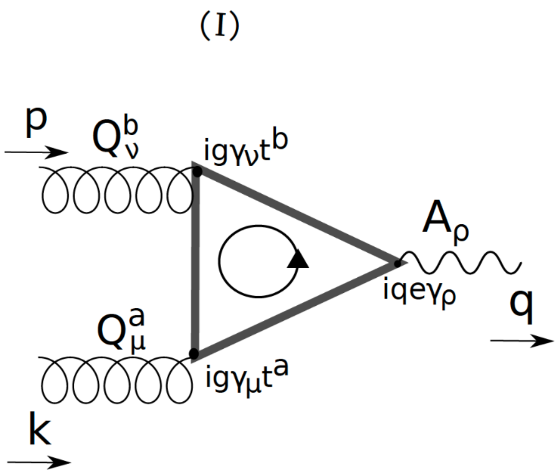

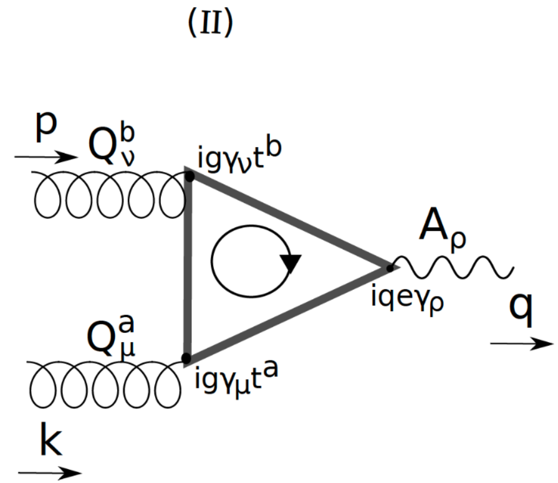

Process diagrams with a triangular quark loop in the presence homogeneous Abelian background gluon field.

p, k denote the gluon momenta, q the photon momentum. Arrows indicate the loop momentum flow.

Within the mean-field approach to the QCD vacuum based on a domain-like structure

Photons production in $gg \to \gamma$ as a signal of deconfinement

- R.P. Feynman, M. Kislinger, F. Ravndal, *Phys. Rev. D* 3 2706-2732 (1971) ;
- H. Leutwyler, J. Stern, *Phys.Lett.B* 73 75-79 (1978) ;
- J. Jersak, H. Leutwyler, J. Stern, *Phys.Lett.B* 77 399-404 (1978) ;
- P. Minkowski, *Nucl.Phys.B* 177, 203-217, (1981) ;
- A.I. Milstein, Yu.F. Pinelis, *Phys.Lett.B* 137 235 (1984) ;

…

Domain-like structure of the QCD vacuum. Key references :

- J. V. Burdanov, G. V. Efimov, S. N. Nedelko, and S. A. Solunin, *Phys. Rev. D* 54, 4483 (1996) ;
- Alex C. Kalloniatis, Sergei N. Nedelko, *Phys. Rev. D* 64, 114025 (2001) ;
- Alex C. Kalloniatis, Sergei N. Nedelko, *Phys. Rev. D* 66, 074020 (2002) ;
- Alex C. Kalloniatis, Sergei N. Nedelko, *Phys. Rev. D* 69, 074029 (2004) ;
- Alex C. Kalloniatis, Sergei N. Nedelko, *Phys. Rev. D 73,* 034006 (2006) ;
- B.V. Galilo and S.N. Nedelko, *Phys. Rev. D* 84, 094017 (2011) ;
- Sergei N. Nedelko and Vladimir E. Voronin, *Eur. Phys. J. A* 51 4, 45 (2015) ;
- Sergei N. Nedelko, Vladimir E. Voronin, *Phys. Rev. D* 93 9, 094010 (2016) ;
- Sergei N. Nedelko, Vladimir E. Voronin, *Phys. Rev. D* 95 7, 074038 (2017) ;
- Sergei N. Nedelko, Vladimir E. Voronin, *Phys. Rev. D* 103 11, 114021 (2021) ;
- Sergei Nedelko, Aleksei Nikolskii, Vladimir Voronin, *J. Phys. G* 49 3, 035003 (2022) ;
- Sergei Nedelko, Vladimir Voronin, *Phys. Rev. D* 107 9, 094027 (2023) ;
- Sergei Nedelko, Aleksei Nikolskii, *Eur. Phys. J. A* 59 4, 70, (2023) ;
- Vladimir Voronin, *Phys. Rev. D* 110 1, 014040 (2024) ;
- Vladimir Voronin, *Phys.Part.Nucl.Lett.* 23 2, 147-154 (2026) ;

…

Photons production in $gg \to \gamma$ as a signal of deconfinement

Domain model of the QCD vacuum and hadronization. Main features.

$$Z = N \int_{\mathcal{F}_B} DA \int_{\Psi} D\Psi D\bar{\Psi} \exp\{-S[A,\psi,\bar{\psi}\,]\}\,,$$

Euclidean QCD functional Integral

$$\mathcal{F}_B = \left\{A\colon \lim_{V\to\infty} \frac{1}{V}\int_V d^4x\, g^2 F^a_{\mu\nu}(x) F^a_{\mu\nu}(x) = B^2\right\},$$

Functional space with a nonzero condensate $\langle g^2 F^2 \rangle$

$$A_\mu \to B_\mu + gQ_\mu\,,$$

Separation of the nonperturbative background field B_μ and perturbative field fluctuations Q_μ

$$D(B)Q = 0\,,$$

Background field gauge

$$1 = \int_{\mathcal{B}} DB\Phi[A,B] \int_Q DQ \int_\Omega D\omega\, \delta[A^\omega - Q^\omega - B^\omega]\, \delta\left[D(B^\omega)Q^\omega\right],$$

$$Z = N' \int_{\mathcal{B}} \mathcal{D}B \int_\Psi \mathcal{D}\psi\mathcal{D}\bar{\psi} \int_Q \mathcal{D}Q \det[D(B)D(B+Q)]\, \delta[D(B)Q] \exp\left\{-S_{\mathrm{QCD}}[B+Q,\psi,\bar{\psi}]\right\} =$$

$$= \int_{\mathcal{B}} \mathcal{D}B\ \exp\{-S_{\mathrm{eff}}[B]\}\,.$$

Definition of the effective action for the field B.

The minima S_{eff} determine different vacuum states of the system in the limit $V \to \infty$.

Photons production in $gg \to \gamma$ as a signal of deconfinement

Domain model of the QCD vacuum and hadronization. Main features.

$$\mathcal{L}_{\text{eff}} = -\frac{1}{4\Lambda^2}\left(D_\nu^{ab}F_{\rho\mu}^{b}D_\nu^{ac}F_{\rho\mu}^{c} + D_\mu^{ab}F_{\mu\nu}^{b}D_\rho^{ac}F_{\rho\nu}^{c}\right) - U_{\text{eff}},$$

Ginzburg–Landau approach to the QCD effective action.

$$U_{\text{eff}} = \frac{\Lambda^4}{12}\,\mathrm{Tr}\left[C_1\left(\frac{\hat F}{\Lambda^2}\right)^2 + \frac{4}{3}C_2\left(\frac{\hat F}{\Lambda^2}\right)^4 - \frac{16}{9}C_3\left(\frac{\hat F}{\Lambda^2}\right)^6\right].$$

U_{eff} has a minimum at $\langle g^2 F_{\mu\nu}^a F_{\mu\nu}^a\rangle \neq 0$ determined by the choice of coefficients C_{i}. The scale $\Lambda \sim \Lambda_{QCD}$ is related to B^2 .

$$D_\mu^{ab} = \delta^{ab}\partial_\mu - i\hat A_\mu^{ab} = \partial_\mu - iA_\mu^c (T^c)^{ab},$$

$$F_{\mu\nu}^a = \partial_\mu A_\nu^a - \partial_\nu A_\mu^a - i f^{abc}A_\mu^b A_\mu^c,$$

$$\hat F_{\mu\nu} = F_{\mu\nu}^a T^a, \qquad T_{bc}^a = -i f^{abc}$$

$$\mathrm{Tr}\,\hat F^2 = \hat F_{\mu\nu}^{ab}\hat F_{\nu\mu}^{ba} = -3F_{\mu\nu}^a F_{\mu\nu}^a \leq 0,$$

$$C_1 > 0, C_2 > 0, C_3 > 0.$$

Definition of symbols

Photons production in $gg \to \gamma$ as a signal of deconfinement

Domain model of the QCD vacuum and hadronization. Main features.

$$\hat{A}_\mu = -\frac{1}{2}\hat{n}_k F_{\mu\nu}x_\nu, \quad \tilde{F}_{\mu\nu} = \frac{1}{2}\varepsilon_{\mu\nu\alpha\beta}F_{\alpha\beta} = \pm F_{\mu\nu}, \quad F_{\mu\nu}F_{\mu\nu} = B^2$$

$U_{\rm eff}$ has twelve degenerate discrete minima for covariantly constant Abelian (anti-)self-dual fields

$$\hat{n}_k = T^3\cos(\xi_k) + T^8\sin(\xi_k), \quad \xi_k = \frac{2k+1}{6}\pi, k = 0,1,\dots,5.$$

The matrix $\hat{n}_k$ belongs to the Cartan subalgebra of the $su(3)$ algebra

$$\vec{E}\vec{H} = B^2\cos(\omega)$$

The angle ω between the chromoelectric and chromomagnetic fields.

$U_{\rm eff}$ for (anti-)self-dual fields in the variables B^2, ξ.

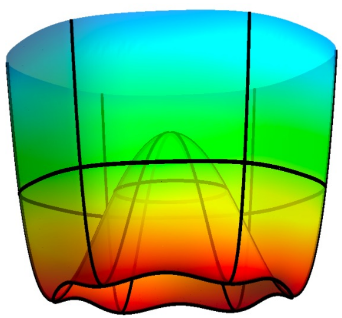

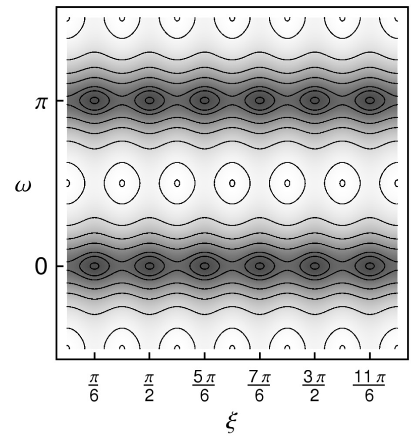

Dependence of $U_{\rm eff}$ on ω and ξ. Dark regions correspond to the minima — Abelian (anti-)self-dual fields.

- Sergei N. Nedelko, Vladimir E. Voronin, *Phys. Rev. D* 93 9, 094010 (2016) ;

Photons production in $gg \to \gamma$ as a signal of deconfinement

Domain model of the QCD vacuum and hadronization. Main features.

Let ξ and $\langle g^2 F^a_{\mu\nu} F^a_{\mu\nu}\rangle$ take their global-minimum values of $U_{\rm eff}$, then for ω one obtains the sine–Gordon equation: $\partial^2\omega = m^2_\omega \sin 2\omega$, $m^2_\omega = b^2_{\rm vac}\,\Lambda^4(C_2 + 3C_3 b^2_{\rm vac})$, which admits kink solutions

$$\omega(x_\nu) = 2\,\mathrm{arctg}\big(\exp(\mu x_\nu)\big).$$

Using an auxiliary function

$$\zeta(\mu_i, \eta^i_\nu x_\nu - q^i) = \frac{2}{\pi}\mathrm{arctg}\left(\exp\left(\mu_i\left(\eta^i_\nu x_\nu \; - \; q^i\right)\right)\right),$$

where μ_i is the inverse kink width, η^i_ν is the normal to the kink plane, and $q^i = \eta^i_\nu x_\nu$ is the wall coordinate, one constructs a superposition of domain-wall pairs

$$\omega(x) = \pi \prod_{i=1}^{k} \zeta(\mu_i, \eta^i_\nu x_\nu - q^i)\,.$$

For a suitable choice of the vectors η^i , such a superposition describes a finite region of anti-self-dual field embedded in a self-dual background in 2, 3, or 4 dimensions for $k = 4,6,8$ respectively.

The general superposition (domain-wall network) is given by:

$$\boxed{\omega(x) = \pi \sum_{j=1}^{\infty} \prod_{i=1}^{k} \zeta(\mu_i, \eta^{ij}_\nu x_\nu - q^{ij}). \qquad (14)}$$

Photons production in $gg \to \gamma$ as a signal of deconfinement

Domain model of the QCD vacuum and hadronization. Main features.

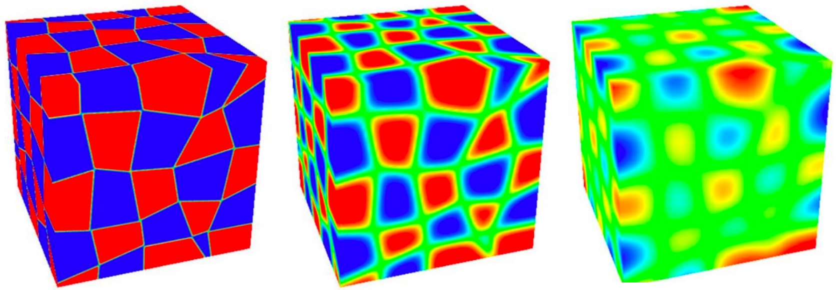

$$\omega(x) = \pi \sum_{j=1}^{\infty} \prod_{i=1}^{k} \zeta(\mu_i, \eta_\nu^{ij} x_\nu - q^{ij}). \qquad (14)$$

$$\langle F^2 \rangle = B^2$$
$$\langle |F\tilde{F}| \rangle = B^2$$

$$\langle F^2 \rangle = B^2$$
$$\langle |F\tilde{F}| \rangle \ll B^2$$

Blue and **red** regions:
confining, almost homogeneous Abelian (anti-)self-dual gluon field.
Confinement.

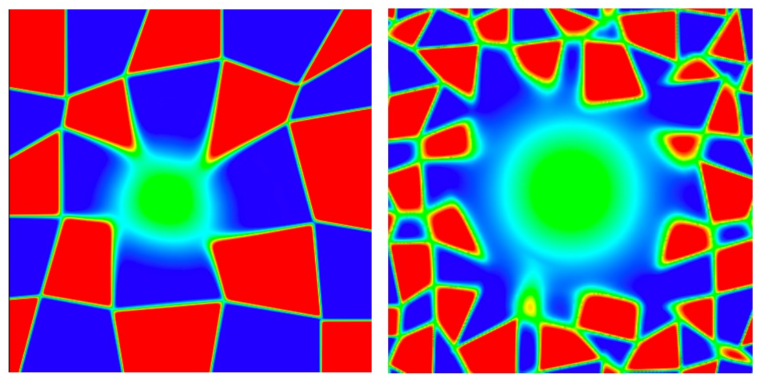

Green regions:
chromomagnetic field where quasiparticles carrying color charge can emerge.
Deconfinement.

- Sergei N. Nedelko and Vladimir E. Voronin, *Eur. Phys. J. A* 51 4, 45 (2015) ;
- B.V. Galilo and S.N. Nedelko, *Phys. Rev. D* 84, 094017 (2011) :

Strong electromagnetic fields produced in heavy-ion collisions can trigger deconfinement.

Photons production in $gg \to \gamma$ as a signal of deconfinement

Domain model of the QCD vacuum and hadronization. Main features.

- Alex C. Kalloniatis, Sergei N. Nedelko, 2001–2006, Refs in slide 28

  Hadronization, confinement, chiral symmetry, propagators and others in domain model are discussed.

- Sergei N. Nedelko, Vladimir E. Voronin, *Phys. Rev. D* 93 9, 094010 (2016) ;

  Mass spectrum and decay constants of radially excited light, heavy-light mesons are presented.

- Sergei N. Nedelko, Vladimir E. Voronin, *Phys. Rev. D* 95 7, 074038 (2017) ;

  Transition form factors $P \to \gamma^*\gamma$ of pseudoscalar mesons are studied.

- Sergei N. Nedelko, Vladimir E. Voronin, *Phys. Rev. D* 103 11, 114021 (2021) ;

  Finite-size domain (R) on the vacuum free energy density of full QCD with N_f massless flavors are studied.

- Sergei Nedelko, Aleksei Nikolskii, Vladimir Voronin, *J. Phys. G* 49 3, 035003 (2022) ;

  HVP and HLbL contributions to muon $g-2$ are discussed.

- B.V. Galilo and S.N. Nedelko, *Phys. Rev. D* 84, 094017 (2011) :

  Strong electromagnetic fields produced in heavy-ion collisions can trigger deconfinement.

- M. D'Elia, M. Mariti, F. Negro, *Phys. Rev. Lett.* 110, 082002 (2013).
- G.S. Bali, F. Bruckmann, G. Endrodi, F. Gruber, A. Schaefer, *JHEP* 04, 130 (2013).

Photons production in $gg \to \gamma$ as a signal of deconfinement

$gg \to \gamma$. Confinement phase

Consider the process $gg \to \gamma$ (via a triangular quark loop) in the presence of a randomly oriented ensemble of almost everywhere homogeneous Abelian (anti-)self-dual domain-structured gluon fields.:

$$\hat{B}_\mu = \frac{1}{2}\hat{B}_{\mu\nu}x_\nu \ , \hat{B}_{\mu\nu} = \hat{n}B_{\mu\nu} \ , \hat{n} = t^8 \, , \tilde{B}_{\mu\nu} = \frac{1}{2}\varepsilon_{\mu\nu\alpha\beta}B_{\alpha\beta} = \pm B_{\mu\nu} \, , \hat{B}_{\rho\mu}\hat{B}_{\rho\nu} = 4v^2B^2\delta_{\mu\nu} \, ,$$

$$\hat{f}_{\alpha\beta} = \frac{\hat{n}}{2vB}B_{\alpha\beta} \ , v = \mathrm{diag}\left(\frac{1}{6}, \frac{1}{6}, \frac{1}{3}\right) \, , \hat{f}^{ik}_{\mu\nu} \, \hat{f}^{kj}_{\nu\alpha} = \delta^{ij}\delta_{\mu\alpha} \, ,$$

where the field strength B sets the scale associated with the scalar gluon condensate. The quark propagator with mass m_f in the presence of the vacuum background field B :

$$(i\gamma_\mu D_\mu - m)S(x,y) = -\delta(x-y) \, , \qquad D_\mu = \partial_\mu - i\hat{B}_\mu \ , \{\gamma_\mu \, , \gamma_\nu\} = -2\delta_{\mu\nu}$$

$$S_f(x,y) = \exp\left(-\frac{i}{2}x_\mu \hat{B}_{\mu\nu}y_\nu\right) H_f(x-y), \tag{15}$$

$$H_f(z) = \frac{vB}{8\pi^2}\int_0^1 \frac{ds}{s^2}\exp\left(-\frac{vB}{2s}z^2\right)\left(\frac{1-s}{1+s}\right)^{\frac{m_f^2}{4vB}} \times$$

$$\left[-i\frac{vB}{s}\, z_\mu \left(\gamma_\mu \pm is\hat{f}_{\mu\nu}\gamma_\nu\gamma_5\right) + m_f\left(P_\pm + \frac{1+s^2}{1-s^2}P_\mp + \frac{i}{2}\gamma_\mu\hat{f}_{\mu\nu}\gamma_\nu\frac{s}{1-s^2}\right)\right].$$

The propagator is an entire function of p^2 .
Quarks do not exist as particle.

❑ B.V. Galilo and S.N. Nedelko, *Phys. Rev. D* 84, 094017 (2011) ;

Photons production in $gg \to \gamma$ as a signal of deconfinement

$gg \to \gamma$. Confinement phase

Terms with odd powers of $\hat{f}$ in the amplitude violate Furry's theorem :

$$M^{(I)} = ieg^2(2\pi)^4\delta^{(4)}(p+k+q)\left(\frac{vB}{8\pi^2}\right)^3 \int_0^1\int_0^1\int_0^1 \frac{ds_1}{s_1^2}\frac{ds_2}{s_2^2}\frac{ds_3}{s_3^2}\frac{(-ivB)^3}{s_1s_2s_3} \tag{16}$$

$$\left(\frac{1-s_1}{1+s_1}\right)^{\frac{m_f^2}{4vB}}\left(\frac{1-s_2}{1+s_2}\right)^{\frac{m_f^2}{4vB}}\left(\frac{1-s_3}{1+s_3}\right)^{\frac{m_f^2}{4vB}}\int d^4x\, d^4y\, e^{-i(px-ky)}$$

$$\left\langle \mathrm{Tr}\ \left[e^{ivBx_\mu\hat{f}_{\mu\nu}y_\nu-\frac{v}{2s_1}x^2-\frac{v}{2s_2}y^2-\frac{v}{2s_3}(y-x)^2}\hat{f}_{\alpha\omega}\hat{f}_{\beta\chi}\hat{f}_{\lambda\eta}K^{\mu\nu\rho}_{\alpha\omega\beta\chi\lambda\eta}+\hat{f}_{\alpha\eta}\hat{f}_{\beta\omega}\Pi^{\mu\nu\rho}_{\alpha\eta}+\hat{f}_{\alpha\omega}\Gamma^{\mu\nu\rho}_{\alpha\omega}\right]\right\rangle \epsilon^a_\mu(k)\epsilon^b_\nu(p)\epsilon_\rho(q),$$

$$M^{(II)} = ieg^2(2\pi)^4\delta^{(4)}(p+k+q)\left(\frac{vB}{8\pi^2}\right)^3 \int_0^1\int_0^1\int_0^1 \frac{ds_1}{s_1^2}\frac{ds_2}{s_2^2}\frac{ds_3}{s_3^2}\frac{(-ivB)^3}{s_1s_2s_3} \tag{17}$$

$$\left(\frac{1-s_1}{1+s_1}\right)^{\frac{m_f^2}{4vB}}\left(\frac{1-s_2}{1+s_2}\right)^{\frac{m_f^2}{4vB}}\left(\frac{1-s_3}{1+s_3}\right)^{\frac{m_f^2}{4vB}}\int d^4x\, d^4y\, e^{-i(px-ky)}$$

$$\left\langle \mathrm{Tr}\ \left[e^{-ivBx_\mu\hat{f}_{\mu\nu}y_\nu-\frac{v}{2s_1}(x-y)^2-\frac{v}{2s_2}y^2-\frac{v}{2s_3}x^2}\hat{f}_{\alpha\omega}\hat{f}_{\beta\chi}\hat{f}_{\lambda\eta}K^{\mu\nu\rho}_{\alpha\omega\beta\chi\lambda\eta}-\hat{f}_{\alpha\eta}\hat{f}_{\beta\omega}\Pi^{\mu\nu\rho}_{\alpha\eta}+\hat{f}_{\alpha\omega}\Gamma^{\mu\nu\rho}_{\alpha\omega}\right]\right\rangle \epsilon^a_\mu(k)\epsilon^b_\nu(p)\epsilon_\rho(q).$$

The amplitudes $M^{(I)}$ and $M^{(II)}$ differ in the **sign** of the phase factor.

Photons production in $gg \to \gamma$ as a signal of deconfinement

$gg \to \gamma$. Confinement phase

The sign in the phase factor affects the result of averaging over the spatial orientation of the background field B

$$\left\langle \prod_{j=1}^{n} \hat{f}_{\alpha_j\beta_j}\, e^{\pm i\hat{f}_{\mu\nu}J_{\mu\nu}} \right\rangle = \frac{(\pm 1)^n}{(2i)^n} \prod_{j=1}^{n} \frac{\partial}{\partial J_{\alpha_j\beta_j}} \frac{\sin\sqrt{2\left(J_{\mu\nu}\, J_{\mu\nu} \pm J_{\mu\nu}\, \tilde{J}_{\mu\nu}\right)}}{\sqrt{2\left(J_{\mu\nu}\, J_{\mu\nu} \pm J_{\mu\nu}\, \tilde{J}_{\mu\nu}\right)}}\,, \tag{18}$$

$$\left\langle \prod_{j=1}^{n} \hat{f}_{\alpha_j\beta_j}\, e^{-i\hat{f}_{\mu\nu}J_{\mu\nu}} \right\rangle = (-1)^n \left\langle \prod_{j=1}^{n} \hat{f}_{\alpha_j\beta_j}\, e^{i\hat{f}_{\mu\nu}J_{\mu\nu}} \right\rangle. \tag{19}$$

Terms in $M = M^{(I)} + M^{(II)}$ containing an even number of $\hat{f}$ cancel each other in analogy with Furry's theorem in QED.

Terms in M with an odd number of $\hat{f}$ cancel after averaging over the orientation of the external field.

The conversion $gg \to \gamma$ is suppressed (vanishes) in a random ensemble of confining vacuum fields.

- Sergei N. Nedelko, Vladimir E. Voronin, *Phys. Rev. D* 95 7, 074038 (2017) ;
- Sergei Nedelko, Aleksei Nikolskii, *Eur. Phys. J. A* 59 4, 70, (2023) ;

Photons production in $gg \to \gamma$ as a signal of deconfinement

$gg \to \gamma$. Deconfinement phase

The deconfinement phase is characterized by the presence of a chromomagnetic field B with a preferred direction (along OZ , i.e., the collision axis):

$$\hat{B}_{\mu\nu} = \hat{n} B_{\mu\nu} = \hat{n} B \, f_{\mu\nu} \, , \;\; f_{12} = - f_{21} = 1 \, . \tag{18}$$

Particle coordinates and momenta (in Euclidean space):

$$x_\perp = (x_1 \, , x_2 \, , 0 \, , 0 \,), \;\; x_\parallel = (0,0, x_3, x_4) \, , \tag{19}$$

$$p_\perp = (p_1 \, , p_2 \, , 0 \, , 0 \,), \;\; p_\parallel = (0,0, p_3, p_4) \, .$$

The quark propagator with mass m_f in the presence of the external chromomagnetic field B (18)

$$S(x,y) = \exp\left\{-\frac{i}{2} x_\perp^\mu \hat{B}_{\mu\nu} y_\perp^\nu\right\} H_f(x-y), \tag{20}$$

The propagator is exact, i.e., it incorporates contributions from all Landau levels.

$$H_f(z) = \frac{B}{16\pi^2} \int_0^\infty \frac{ds}{s} \left\{ m_f - \frac{i}{2s} \gamma_\mu z_\parallel^\mu - \frac{1}{2} \gamma_\mu \hat{B}_{\mu\nu} z_\perp^\nu - \frac{i}{2} B|\hat{n}| \coth(B|\hat{n}|s) \gamma_\mu z_\perp^\mu \right\}$$

$$\left[|\hat{n}| \coth(B|\hat{n}|s) - \frac{1}{2} \sigma_{\rho\lambda} f_{\rho\lambda} \right] \exp\left\{ -m_f^2 s - \frac{1}{4s} z_\parallel^2 - \frac{1}{4} B|\hat{n}| \coth(B|\hat{n}|s) \gamma_\mu z_\perp^2 \right\} ,$$

$$\sigma_{\rho\lambda} = \frac{i}{2i} [\gamma_\rho \, , \gamma_\lambda] \, .$$

Photons production in $gg \to \gamma$ as a signal of deconfinement

$gg \to \gamma$. Deconfinement phase

The amplitude for diagrams (I) и (II):

$$M = M^{(I)} + M^{(II)} = i(2\pi)^4\delta^4(p+k-q)g^2e\sum_l \mathcal{F}^l_{\mu\nu\rho}(p,k)F_l(p,k)\delta^{a8}\delta^{b8}\epsilon^a_\mu(k)\epsilon^b_\nu(p)\epsilon_\rho(q). \tag{21}$$

The form factors F_l have the following structure:

$$F_l(p,k) = \sum_f q_f \,\mathrm{Tr}_{\hat n} \int_0^\infty ds_1 ds_2 ds_3 \left[\psi_l^{(I)}(s_1,s_2,s_3|\hat n, m_f) + \psi_l^{(II)}(s_1,s_2,s_3|\hat n, m_f)\right] \tag{22}$$

$$\times\exp\{-p_\parallel^2\phi_1(s_1,s_2,s_3) - p_\parallel k_\parallel\phi_2(s_1,s_2,s_3) - k_\parallel^2\phi_3(s_1,s_2,s_3)$$

$$-p_\perp^2\phi_4(s_1,s_2,s_3) - p_\perp k_\perp\phi_5(s_1,s_2,s_3) - k_\perp^2\,\phi_6(s_1,s_2,s_3) - m_f^2(s_1,s_2,s_3)\}.$$

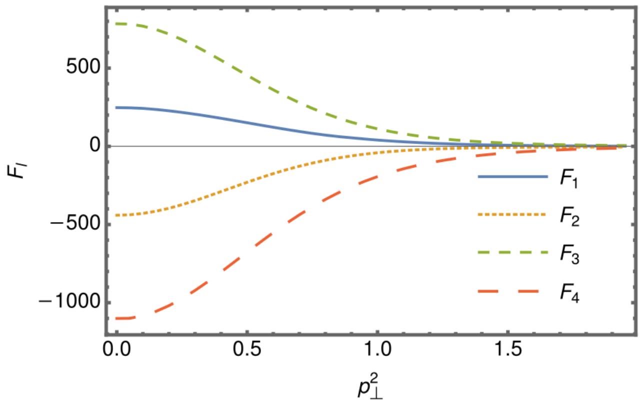

Some form factors of the amplitude M as functions of $p_\perp^2 = k_\perp^2$ at $p_\parallel^2 = k_\parallel^2 = 1$ in Euclidean kinematics. $\boldsymbol{\phi_1, .., \phi_6 > 0}$.
The form factors are dimensionless, with, $p^2 = p^2/B$.

The amplitude contains 32 form factors.

❑ Sergei Nedelko, Aleksei Nikolskii, *Eur. Phys. J. A* 59 4, 70, (2023)

$gg \to \gamma$. Deconfinement phase

To evaluate $T = |M|^2$ an analytic continuation to Minkowski space is required:

$$p_\parallel^2 \to -p_\parallel^2\,,\;\; k_\parallel^2 \to -k_\parallel^2\,,\;\; p_\parallel k_\parallel \;\to -p_\parallel k_\parallel\,. \tag{23}$$

In Minkowski kinematics, the on-shell conditions for the gluons and the photon lead to the relations:

$$p_\parallel^2 = p_\perp^2\,,\;\; k_\parallel^2 = k_\perp^2\,,\;\; p_\parallel k_\parallel = p_\perp k_\perp\,. \tag{24}$$

The photon production probability is determined by the squared amplitude, averaged over the initial gluon polarization states and summed over the final photon polarizations:

$$\boxed{\bar{T}(p,k,q) = \Delta\nu\Delta\tau(2\pi)^4\delta^4(p+k-q)T(p,k)\,,} \tag{25}$$

$$T(p,k) = \frac{2\alpha\alpha_s}{\pi}\int ds_1 ds_2 ds_3 dr_1 dr_2 dr_3 F(s_1,s_2,s_3,r_1,r_2,r_3|p,k)$$

$$\times\exp\{\, p_\perp^2\Phi_1(s_1,s_2,s_3,r_1,r_2,r_3) + p_\perp k_\perp\Phi_2(s_1,s_2,s_3,r_1,r_2,r_3) + k_\perp^2\,\Phi_3(s_1,s_2,s_3,r_1,r_2,r_3)$$
$$-m_f^2(s_1,s_2,s_3,r_1,r_2,r_3)\,\}.$$

Photons production in $gg \to \gamma$ as a signal of deconfinement

$gg \to \gamma$. Deconfinement phase

The functions

$$\Phi_1(s_1,s_2,s_3,r_1,r_2,r_3) = \phi_1(s_1,s_2,s_3) + \phi_1(r_1,r_2,r_3) - \phi_4(s_1,s_2,s_3) - \phi_4(r_1,r_2,r_3)\,, \tag{26}$$

$$\Phi_2(s_1,s_2,s_3,r_1,r_2,r_3) = \phi_2(s_1,s_2,s_3) + \phi_2(r_1,r_2,r_3) - \phi_5(s_1,s_2,s_3) - \phi_5(r_1,r_2,r_3)\,,$$

$$\Phi_3(s_1,s_2,s_3,r_1,r_2,r_3) = \phi_3(s_1,s_2,s_3) + \phi_3(r_1,r_2,r_3) - \phi_6(s_1,s_2,s_3) - \phi_6(r_1,r_2,r_3)\,.$$

are positive over the entire integration region and grow linearly as $s_j \to \infty$. The proper-time integrals in Eq. (25) «converge» only within a limited range of momenta p, k, q determined by the quark mass m_f . For the kinematic regime $p_\perp^2 = k_\perp^2 = q^2/4$ the integrals over s_j converge provided that

$$\boxed{p_\perp^2 < \frac{3}{2} m_f^2 \leftrightarrow q^2 < 6\, m_f^2\,.} \tag{27}$$

Similar features of «photon splitting» have been discussed in:

- S.L. Adler, J.N. Bahcall, C.G. Callan, and M.N. Rosenbluth, *Photon spliting in a strong magnetic field*, Phys. Rev. Lett. 25, 1061 (1970) ;
- V.O. Papanyan and V.I. Ritus, *Vacuum polarization and photon splitting in an intense fiield*, Zh. Eksp. Teor. Fiz. 61, 2231 (1971) ;
- V.O. Papanyan and V.I. Ritus, *Three-photon interaction in an intense field and scaling invariance*, Zh. Eksp. Teor. Fiz. 65, 1756 (1973) ;

Photons production in $gg \to \gamma$ as a signal of deconfinement

$gg \to \gamma$. Deconfinement phase

In the papers

- A. Ayala et al. *Phys. Rev. D* 96, 014023 (2017) ;
- A. Ayala et al. *Eur. Phys. J. A* 56 , 53 (2020) ;

the conversion process $gg \to \gamma$ was studied under the following assumptions:

- the strong (pure magnetic) field limit: $eB_{\mathrm{el}} \gg m_f^2$;
- massless quarks ;
- quark propagators restricted to the lowest (LLL) and first excited (1LL) Landau levels.

In this case, the photon production probability for $gg \to \gamma$

$$\boxed{T_{B_{\mathrm{el}}}(p,k) = \frac{2\alpha\alpha_s^2}{\pi} q_f^2 (2p_\perp^2 + k_\perp^2 + p_\perp k_\perp)\exp\left\{-\frac{1}{|q_f B_{\mathrm{el}}|}(p_\perp^2 + k_\perp^2 + p_\perp k_\perp)\right\}.} \tag{28}$$

To estimate the effect of the chromomagnetic field over a broad momentum range p, k, q , we generalize the result by the replacement: $|q_f B_{\mathrm{el}}| \longrightarrow |q_f B_{\mathrm{el}} + \hat{n}B|$. This yields:

$$\boxed{T_B(p,k) = \frac{2\alpha\alpha_s^2}{\pi} q_f^2 \,\mathrm{Tr}_{\hat{n}}\, (2p_\perp^2 + k_\perp^2 + p_\perp k_\perp)\exp\left\{-\frac{1}{|q_f B_{\mathrm{el}} + \hat{n}B|}(p_\perp^2 + k_\perp^2 + p_\perp k_\perp)\right\}.} \tag{29}$$

Photons production in $gg \to \gamma$ as a signal of deconfinement

$gg \to \gamma$. Deconfinement phase

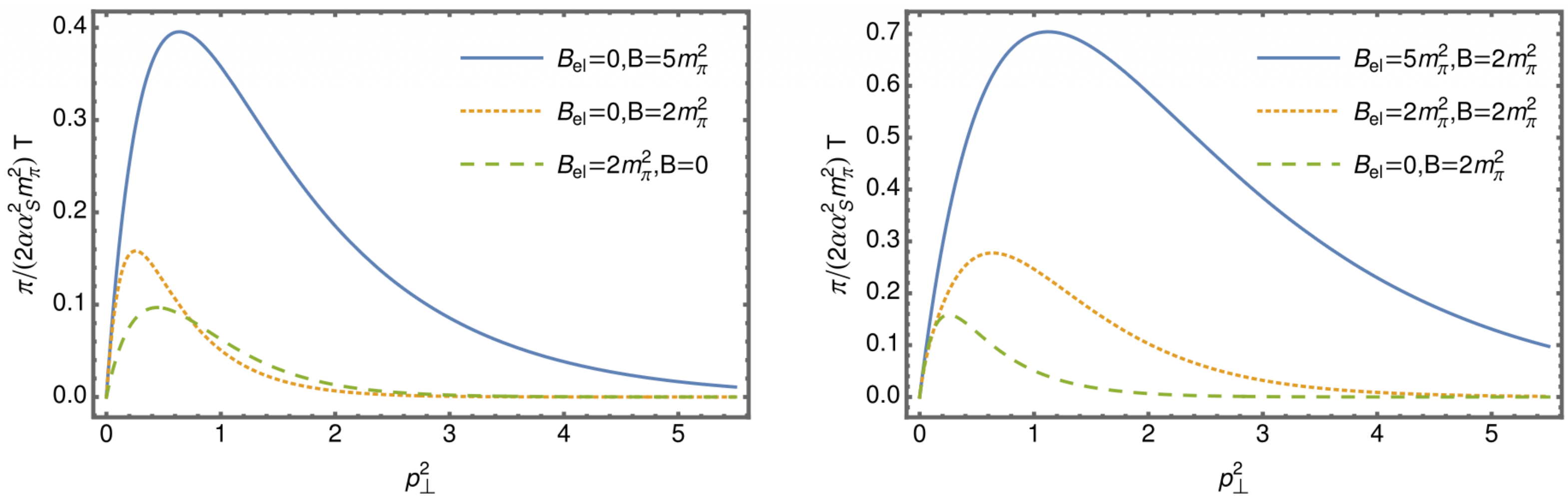

Dependence of $T(p, k)$, Eqs. (28) and (29) on the different fields B and B_{el} for $p_\perp^2 = k_\perp^2 = q^2/4$. The pion mass m_π is used as the scale parameter, and the momenta are expressed in dimensionless units $p^2 = p^2/B$.

Left: the effect of the chromomagnetic field B is stronger than that of the purely magnetic field B_{el} (orange and green curves).
Right: photon production is enhanced by the «long lifetime» of the chromomagnetic field.

❑ Sergei Nedelko, Aleksei Nikolskii, *Eur. Phys. J. A* 59 4, 70, (2023) .

Photons production in $gg \to \gamma$ as a signal of deconfinement

$gg \to \gamma$. Deconfinement phase

Invariant differential photon spectrum in the presence of magnetic and chromomagnetic fields B_{el} and B, respectively :

$$\frac{1}{2\pi\omega_q}\frac{dN}{d\omega_q} = \nu\Delta\tau\frac{\alpha\alpha_s^2\pi}{2N_c(2\pi)^6\omega_q} q_f^2 \,\mathrm{Tr}_{\hat{n}} \int_0^{\omega_q} d\omega_p\left(2\omega_p^2+\omega_q^2-\omega_p\omega_q\right)\, e^{-g_f^B(\omega_p,\omega_q)} \tag{30}$$

$$\times\left[I_0\left(g_f^B(\omega_p,\omega_q)\right)-I_1\left(g_f^B(\omega_p,\omega_q)\right)\right]\left[n(\omega_p)n(|\omega_q-\omega_p|)\right],$$

where $g_f^B(\omega_p,\omega_q)=\frac{\omega_p^2+\omega_q^2-\omega_p\omega_q}{2|\hat{n}B+q_fB_{el}|}$, $n(\omega)=\eta/(e^{\frac{\omega}{\Lambda_s}}-1)$, I_0 , I_1 are the modified Bessel functions of the first kind.

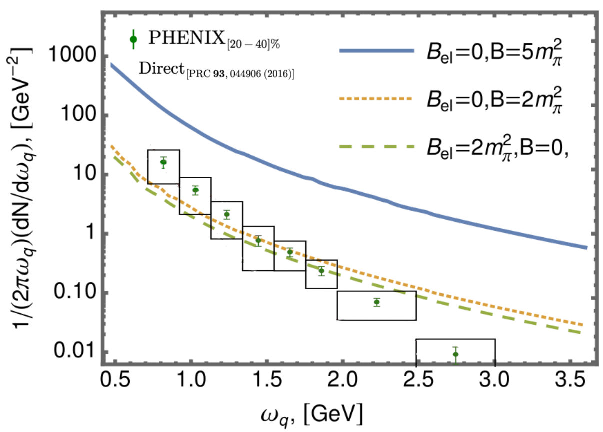

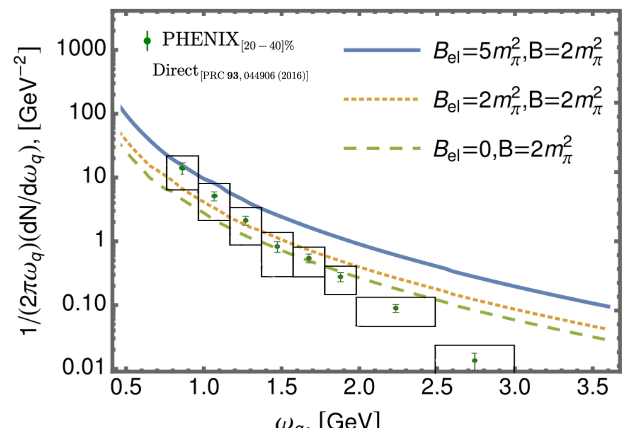

Notation is the same as in the previous figure.

Photons production in $gg \to \gamma$ as a signal of deconfinement

$gg \to \gamma$. Deconfinement phase

In the momentum range $p_\perp^2 = k_\perp^2 < \frac{3}{2} m_f^2$ (or $q^2 < 6\, m_f^2$) the photon production probability can be compared for the following cases: using the «full» quark propagator, Eq. (25); using the Landau-level expansion, Eq. (29):

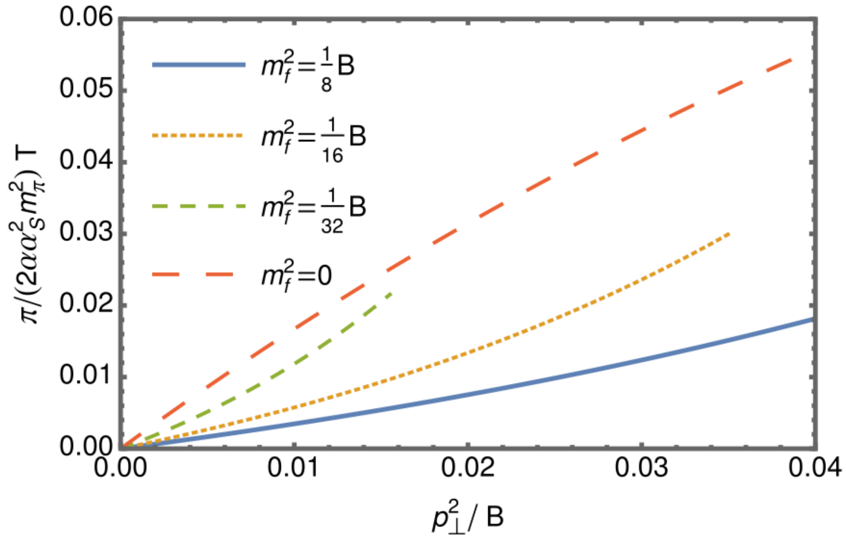

$m_{u/d}$ (MeV)	m_s (MeV)	m_c (MeV)	m_b (MeV)	Λ (MeV)	α_s	R (fm)
145	376	1566	4879	416	3.45	1.12

- Sergei N. Nedelko, Vladimir E. Voronin, *Phys. Rev. D* 95 7, 074038 (2017) ;

The chromomagnetic field is fixed at $B = 4m_\pi^2$.

Similar «difficulties» associated with the integral representation arise in the region $m_f^2 < |q_f B_{el}| < q^2$ when all quark Landau levels are included:

- A. Ayala et al. *Phys. Rev. D* 110 7, 076021 (2024) .

Photons production in $gg \to \gamma$ as a signal of deconfinement

- Photon production via the process $gg \to \gamma$ (through a triangular quark loop) may serve as a signal of the confinement–deconfinement phase transition ;

- Confinement phase: the probability of two-gluon conversion into a photon vanishes due to the random orientation of the statistical ensemble of confining vacuum fields ;
- Deconfinement phase: the short-lived magnetic field generated in heavy-ion collisions acts as a catalyst for the transition to deconfinement. This transition is accompanied by the emergence of a long-lived chromomagnetic field aligned with the magnetic field. As a result, Furry's theorem is violated, and the conversion probability $gg \to \gamma$ becomes nonzero ;

- For massless quarks, the chromomagnetic field enhances the photon production amplitude owing to both its strength and its longer lifetime ;
- Proper treatment of quark masses is important, especially for the $s-$quark, for which the Landau-level expansion is not applicable ;

- The produced photons exhibit a pronounced angular anisotropy because the amplitude depends on the preferred direction defined by the external (chromo)magnetic field.

Conclusions

Synchrotron radiation from quarks

- Photon production via synchrotron radiation from quarks is a consequence of (de)confinement in the QGP;
- The relative contribution of this mechanism can reach 10% or more of the experimentally observed photon yield;
- The polarization of synchrotron photons induces an azimuthal anisotropy of the resulting dilepton pairs;
- Synchrotron photons contribute to the overall direct-photon elliptic flow $v_2^{\gamma\ \mathrm{dir}}$;

Photons from $gg \to \gamma$ as a signal of deconfinement

- Photon production via the process $gg \to \gamma$ (through a triangular quark loop) may serve as a signal of the confinement–deconfinement phase transition ;
- Confinement phase: the probability of two-gluon conversion into a photon vanishes because of the random orientation of the statistical ensemble of confining vacuum fields ;
- Deconfinement phase: a «long-lived» chromomagnetic field with a preferred direction emerges. As a consequence, Furry's theorem is violated, and the conversion probability $gg \to \gamma$ becomes nonzero ;
- The produced photons exhibit a strong angular anisotropy since the amplitude depends on the preferred direction of the external (chromo)magnetic fields.

Thank you for your attention !

BACKUP BACKUP BACKUP

BACKUP

Publications Related to This Talk

- V.V. Goloviznin, A.V. Nikolskii, A.M. Snigirev, and G.M. Zinovjev, *Eur. Phys. J. A* 55: 142, (2019), arXiv: 1804.00559 ;
- V.V. Goloviznin, A.V. Nikolskii, A.M. Snigirev, and G.M. Zinovjev, *PoS HardProbes 2018* (2018) 175 Contribution to: HP2018, 175 ;
- S. Nedelko, A. Nikolskii, *Eur. Phys. J. A* 59 4, 70, (2023), arXiv: 2208.00842 ;
- Sergei Nedelko, Aleksei Nikolskii, *MDPI Physics 5* (2023) 2, 547-553 ;
- S. N. Nedelko, A. V. Nikolskii, *Phys.Part.Nucl.Lett. 20* (2023) 5, 1153-1156 ;

Presentations Related to This Work

- “Synchrotron radiation as a probe of confinement and QGP”, Hard Probes 2018: International Conference on Hard and Electromagnetic Probes of High-Energy Nuclear Collisions, 30 September – 5 October 2018, CERN, Aix-Les-Bains, France;
- “Synchrotron radiation in quark-gluon plasma”, International conference of students, graduate students and young scientists "Lomonosov-2019", 8-12 April 2019, Moscow, Russia;
- “Electromagnetic radiation in heavy-ion collisions and deconfinement phase”, IV International Scientific Forum “Nuclear science and Technologies”, 26-30 September 2022, Almaty, Republic of Kazakhstan;
- “Photons production in heavy-ion collisions as a signal of deconfinement phase”, The XXVI International Scientific Conference of Young Scientists and Specialists (AYSS-2022), 24-28 October 2022, Dubna, Russian Federation;
- “Photons as a signal of deconfinement in hadronic matter under extreme conditions”, The 6th international conference on particle physics and astrophysics (ICPPA-2022), 29 November - 2 December 2022, Moscow, Russian Federation;

Some general facts

$$A\mu = B\mu + Q\mu$$

↓

вставка единицы (обобщённое тождество Фаддеева–Попова)

$$\delta[A - B - Q]\,\delta[D(B)Q]$$

↓

условие фоновой калибровки

$$D\mu(B)Q\mu = 0$$

↓

оператор Фаддеева–Попова

$$M^{ab} = \frac{\delta G^a}{\delta \omega^b} = [D(B)D(B+Q)]^{ab}$$

↓

детерминант

$$\det[D(B)D(B+Q)]$$

↓

гхосты $c, \bar{c}$

↓

интегрирование по $Q, \psi, \bar{\psi}, c, \bar{c}$

↓

эффективное действие

$$S\text{eff}[B]$$

↓

минимумы $S\text{eff}$

↓

вакуумные конфигурации (домены).

Что означает эта формула физически?

Она говорит:

1. выбираем фоновую конфигурацию B;
2. рассматриваем все квантовые флуктуации Q вокруг неё;
3. рассматриваем все кварковые поля;
4. учитываем фактор Фаддеева–Попова;
5. затем усредняем по всем допустимым фонам B.

В записи

$$G^a(x) = D\mu^{ab}(B)\,Q\mu^b(x)$$

G^a — это просто **калибровочная функция** (gauge-fixing function), задающая условие калибровки.

В фоновой калибровке выбирают

$$G^a = D\mu^{ab}(B)Q\mu^b = 0.$$

Это аналог лоренцевой калибровки в КЭД

$$G = \partial\mu A\mu = 0.$$

Где появляются гхосты?

Гхосты возникают из детерминанта Фаддеева–Попова

$$\det\left(\frac{\delta G^a}{\delta \omega^b}\right).$$

Для фоновой калибровки

$$G^a = D\mu^{ab}(B)Q\mu^b,$$

поэтому

$$\frac{\delta G^a}{\delta \omega^b} = \left[D(B)D(B+Q)\right]^{ab}.$$

Отсюда и появляется в твоей формуле

$$\det[D(B)D(B+Q)].$$

Где появляются гхосты?

Гхосты возникают из детерминанта Фаддеева–Попова

$$\det\left(\frac{\delta G^a}{\delta \omega^b}\right).$$

Для фоновой калибровки

$$G^a = D\mu^{ab}(B)Q\mu^b,$$

поэтому

$$\frac{\delta G^a}{\delta \omega^b} = \left[D(B)D(B+Q)\right]^{ab}.$$

Отсюда и появляется в твоей формуле

$$\det[D(B)D(B+Q)].$$

Затем этот детерминант обычно представляют через антикоммутирующие скалярные поля

$$c^a, \qquad \bar{c}^a,$$

которые и называются **духами (ghosts) Фаддеева–Попова**:

$$\det[D(B)D(B+Q)] = \int Dc\, D\bar{c}\, e^{-S\text{ghost}}.$$

При этом

$$S\text{ghost} = \int d^4x\, \bar{c}^a \left[D(B)D(B+Q)\right]^{ab} c^b.$$

BACKUP

1. Обычный интеграл и функциональный интеграл

В обычной квантовой механике вероятность получить величину вычисляется через интеграл по переменным:

$$\int dx\, e^{-S(x)}.$$

В квантовой теории поля вместо одной переменной x есть целое поле $A_\mu(x)$, определённое в каждой точке пространства-времени.

Поэтому вместо суммы по числам возникает сумма по всем возможным конфигурациям поля:

$$\int \mathcal{D}A\, e^{-S[A]}.$$

Символ

$$\mathcal{D}A$$

означает:

> «проинтегрировать по всем возможным функциям $A_\mu(x)$».

2. Производящий функционал КХД

Для КХД

$$Z = \int \mathcal{D}A\, \mathcal{D}\bar{q}\, \mathcal{D}q\, e^{-S_{QCD}[A,\bar{q},q]}.$$

Здесь учитываются одновременно:

- все глюонные поля A_μ;
- все кварковые поля q;
- все поля $\bar{q}$.

То есть вакуум КХД — это не одна конфигурация, а суперпозиция бесконечного числа конфигураций.

3. Среднее значение оператора

Если есть оператор O, то его вакуумное среднее:

$$\langle O \rangle = \frac{1}{Z} \int \mathcal{D}A\, \mathcal{D}\bar{q}\, \mathcal{D}q\, O\, e^{-S}.$$

Это просто аналог статистической физики:

$$\langle O \rangle = \frac{\sum O\, e^{-E/T}}{\sum e^{-E/T}}.$$

Только вместо суммы по состояниям — функциональный интеграл по полям.

Some general facts

4. Почему появляются детерминанты?

Кварковое действие имеет вид

$$S_q = \int d^4x\, \bar{q}(i \not{D} - m) q.$$

Оно квадратично по кварковым полям.

Аналог обычной формулы

$$\int dx\, e^{-ax^2} \propto a^{-1/2}.$$

Для фермионов получается

$$\int \mathcal{D}\bar{q}\, \mathcal{D}q\, e^{-\bar{q}Mq} = \det M.$$

Поэтому

$$\int \mathcal{D}\bar{q}\, \mathcal{D}q\, e^{-\bar{q}(\not{D}-m)q} = \det(i \not{D} - m).$$

Это одна из самых важных формул в КХД.

5. Почему возникает $\ln \det$?

Потому что

$$\det M = e^{\ln \det M}.$$

Тогда

$$Z = \int \mathcal{D}A\, e^{-S_g[A]} \det(i \not{D} - m)$$

можно переписать как

$$Z = \int \mathcal{D}A\, e^{-S_g[A] + \ln \det(\not{D} - m)}.$$

Отсюда

$$S_{\text{eff}} = S_g - \ln \det(i \not{D} - m).$$

Some general facts

6. Почему $\ln\det$ — это кварковые петли?

Используется тождество

$$\ln\det M = \mathrm{Tr}\,\ln M.$$

Пусть

$$M = M_0 + V.$$

Тогда

$$\mathrm{Tr}\ln(M_0+V) = \mathrm{Tr}\ln M_0 + \sum_{n=1}^{\infty}\frac{(-1)^{n+1}}{n}\mathrm{Tr}(M_0^{-1}V)^n.$$

Каждый член

$$\mathrm{Tr}(M_0^{-1}V)^n$$

соответствует замкнутой кварковой петле с n внешними глюонами.

Поэтому

$$\ln\det(i\not{D}-m)$$

есть сумма всех однопетлевых кварковых диаграмм.

7. Откуда берётся пропагатор?

Ещё одно важное тождество:

$$d\ln\det M = \mathrm{Tr}(M^{-1}dM).$$

Для

$$M = i\not{D}-m$$

получаем

$$M^{-1} = (i\not{D}-m)^{-1} \equiv S.$$

То есть производная функционального детерминанта автоматически приводит к кварковому пропагатору.

Именно поэтому:

$$\langle\bar{q}q\rangle = -\mathrm{Tr}\,S,$$

а вариации эффективного действия содержат кварковые токи.

8. Что важно помнить для доменной модели?

Можно свести всё к трём строкам:

$$Z = \int \mathcal{D}A\,\mathcal{D}\bar{q}\,\mathcal{D}q\,e^{-S_{QCD}}$$

$$\Downarrow \quad \text{интегрирование по кваркам}$$

$$Z = \int \mathcal{D}A\,e^{-S_g+\ln\det(\not{D}-m)}$$

$$\Downarrow \quad \text{эффективное действие}$$

$$S_{\mathrm{eff}}[A] = S_g[A] - \ln\det(i\not{D}-m).$$

После этого ищут минимумы S_{eff}, строят доменную структуру вакуума, а затем изучают кварки уже в найденном фоновом поле.

Для большинства статей Неделко, Воронова и соавторов именно эта цепочка является центральной: **функциональный интеграл → детерминант Дирака → эффективное действие → вакуумное поле → свойства кварков и адронов**.

2. Физический (непертурбативный) вакуум

В нём присутствуют вакуумные средние различных операторов:

$$\langle\bar{q}q\rangle \neq 0,$$

$$\left\langle\frac{\alpha_s}{\pi}G^a_{\mu\nu}G^a_{\mu\nu}\right\rangle \neq 0,$$

$$\langle q(x)q(0)\rangle \neq 0,$$

и т.д.

То есть вакуум КХД — это не пустота, а сложная среда.

BACKUP

Some general facts

$$\mathcal{L}_{QCD} \to Z \to S_{\text{eff}} \to U_{\text{eff}} \to \text{вакуум}$$

а дальше

$$\text{вакуум} \to \langle \bar{q}q \rangle,\ \langle G^2 \rangle,\ \chi,\ \text{мезоны},\ \text{конфайнмент}.$$

Если оставить только самое главное для семинара или быстрого объяснения:

1. **Вакуум КХД** — это состояние с минимальной энергией.
2. Энергия извлекается из функционального интеграла:

$$E_{\text{vac}} = -\lim_{\beta\to\infty} \frac{1}{\beta} \ln Z.$$

3. После интегрирования по кваркам:

$$S_{\text{eff}} = S_g - \ln\det(i\not{D} - m).$$

4. Для однородных фоновых полей:

$$S_{\text{eff}} = V_4 U_{\text{eff}}.$$

5. Минимум U_{eff} определяет вакуумное поле.
6. В этом вакууме вычисляются конденсаты и свойства адронов.

Подалгебра Картана группы $SU(3)$ — это двумерная коммутирующая подалгебра, натянутая на генераторы T^3 и T^8. В доменной модели фоновое глюонное поле выбирается направленным вдоль этой подалгебры, что делает его эффективно абелевым и позволяет аналитически вычислять спектры и эффективное действие.

У группы $SU(3)$ есть восемь генераторов

$$T^a = \frac{\lambda^a}{2}, \qquad a = 1,\dots,8.$$

Среди них коммутируют

$$T^3, \qquad T^8.$$

Действительно,

$$[T^3, T^8] = 0.$$

Они образуют подалгебру Картана:

$$\mathfrak{h} = \{T^3, T^8\}.$$

Ранг группы

$$\operatorname{rank}(SU(3)) = 2.$$

В доменной модели фоновое поле обычно выбирают абелевым:

$$\hat{n} = n^a T^a,$$

где $\hat{n}$ лежит именно в подалгебре Картана.

То есть

$$\hat{n} = \cos\theta\, T^3 + \sin\theta\, T^8.$$

или эквивалентно через диагональные матрицы Гелл-Манна.

Тогда фоновое поле записывают как

$$B^a_{\mu\nu} = n^a B_{\mu\nu}.$$

Some general facts

Когда в статьях пишут

$$\hat{n} = T^3 \cos\xi + T^8 \sin\xi,$$

это не просто технический приём. По сути авторы выбирают направление фонового цветового поля в двумерном пространстве Картана. Аналогия такая:

- в обычной электродинамике магнитное поле имеет направление в физическом пространстве;
- в КХД фоновое поле имеет ещё и направление в **цветовом пространстве**;
- подалгебра Картана задаёт удобную «цветовую плоскость», в которой это направление можно параметризовать одним углом ξ.

Поэтому параметры

$$B, \quad R, \quad \xi$$

в доменной модели имеют простой смысл:

- B — напряжённость фонового поля;
- R — размер домена;
- ξ — направление поля в цветовом пространстве Картана.

А дискретные значения

$$\xi_k = \frac{(2k+1)\pi}{6}$$

появляются уже из минимизации свободной энергии и отражают симметрию группы $SU(3)$.

Представление	На что действует	Размер матриц
Фундаментальное	кварки q	3×3
Присоединённое	глюоны A^a	8×8

$$(T^a_F) = \frac{\lambda^a}{2}, \qquad (T^a_A)_{bc} = -if^{abc}.$$

И эксперименты:

- RHIC
- LHC

дают значения близкие к:

$$\eta/s \sim 0.1 - 0.2$$

то есть очень близко к $1/(4\pi) \approx 0.08$.

4. Физическая картинка

Можно думать так:

- кварки и глюоны не свободны
- они образуют сильно взаимодействующую “суповую” среду
- импульс быстро перераспределяется через многократные столкновения

→ отсюда почти идеальная гидродинамика